





# Sticky PDMP samplers for sparse and local inference problems

Joris Bierkens <sup>1</sup>, Sebastiano Grazi <sup>1</sup>,  
Frank van der Meulen <sup>1</sup>, and Moritz Schauer <sup>2</sup>

<sup>1</sup>Delft Institute of Applied Mathematics (DIAM), Delft University of Technology

<sup>2</sup>Department of Mathematical Sciences, Chalmers University of Technology and University of Gothenburg

April 24, 2022

## Abstract

We construct a new class of efficient Monte Carlo methods based on continuous-time piecewise deterministic Markov processes (PDMPs) suitable for inference in high dimensional sparse models, i.e. models for which there is prior knowledge that many coordinates are likely to be exactly 0. This is achieved with the fairly simple idea of endowing existing PDMP samplers with sticky coordinate axes, coordinate planes etc. Upon hitting those subspaces, an event is triggered, during which the process *sticks* to the subspace, this way spending some time in a sub-model. That introduces *non-reversible* jumps between different (sub-)models. The approach can also be combined with local implementations of PDMP samplers to target measures that additionally exhibit a sparse dependency structure. We illustrate the new method for a number of statistical models where both the sample size  $N$  and the dimensionality  $d$  of the parameter space are large.

*Keywords:* variable selection, piecewise deterministic Markov process, Monte Carlo, spike-and-slab, big-data, high-dimensional problems, non-reversible jump

## 1 Introduction

Consider the problem of simulating from a measure  $\mu$  on  $\mathbb{R}^d$  that is a mixture of atomic and continuous components. A key application is Bayesian inference for sparse problems and variable selection under a spike-and-slab prior  $\mu_0$  of the form

$$\mu_0(dx) = \prod_{i=1}^d (w_i \pi_i(x_i) dx_i + (1 - w_i) \delta_0(dx_i)). \quad (1.1)$$

Here,  $w_i \in [0, 1]$ ,  $\pi_1, \pi_2, \dots, \pi_d$  are densities referred to as *slabs* and  $\delta_0$  denotes the Dirac measure at zero. A common sampling technique is to construct and simulate a Markov process that has  $\mu$  as invariant measure. Standard samplers requiring (the gradient of) a density with respect to the Lebesgue measure, for example the popular Hamiltonian Monte Carlo sampler (Duane et al., 1987), cannot be directly applied due to the degenerate nature of  $\mu$ .

We show that samplers based on piecewise deterministic Markov processes (PDMPs) can be adapted to sample from such mixture measures by introducing *stickiness*. Here the process can spend a positive amount of time at the origin, at the coordinate axes and at the coordinate (hyper-)planes by sticking to 0 in each coordinate for a random time span whenever the process hits 0 in that particular coordinate. PDMPs have received recent attention because they have good mixing properties (they are non-reversible and they have ‘momentum’), they take gradient information into account and they are attractive in Bayesian inference scenarios with a large number of observations because they allow for subsampling of the observations without creating bias.

By introducing stickiness, we generalize PDMPs for sampling mixture measures *without losing momentum or introducing random walk behaviour* and effectively generating *non-reversible jumps between states with different sets of non-zero coordinates (models)*. We cover several well known PDMP samplers: the Zig-Zag sampler (Bierkens, Fearnhead, and Roberts, 2019), the Bouncy Particle sampler (Bouchard-Côté, Vollmer, and Doucet, 2015) and the Boomerang sampler (Bierkens et al., 2020), the latter having Hamiltonian deterministic dynamics invariant to a prescribed Gaussian measure. As a result, we extend, for example, the application of PDMPs to Bayesian inference with a large number of observations ( $N$ ) and/or parameters ( $d$ ). The problems with large  $d$  (and large  $N$ ) are critical in Bayesian computations since most of the state-of-the-art algorithms have shown limitations in this setting, see Chopin and Ridgway (2015, Section 7) for a discussion.

In piecewise deterministic Markov processes, the state space is augmented by adding to each coordinate  $x_i$  a velocity or momentum component  $v_i$ , doubling the dimension of the state space. They are characterized by piecewise deterministic dynamics between event times, where (depending on the sampler) event times correspond to change of velocities (reflection), or a refreshment of the velocities to ensure mixing of the process.

We introduce “sticking event” times, which occur every time a coordinate of the process state passes through the point 0. At such time that particular component of the state freezes for an independent exponentially distributed time with rate  $|v_i|\kappa_i$ , for some  $\kappa_i > 0$ . This corresponds to temporarily setting the marginal velocity to 0: the process “sticks to (or freezes at) 0” in that coordinate, while the other coordinates keep moving, as long as they are not stuck themselves. After the exponentially distributed time the coordinate moves again with its original velocity. Figure 1 illustrates a prototypical trajectory of the 2-dimensional sticky Zig-Zag process.

This allows us to construct a piecewise deterministic process that has a pre-specified measure  $\mu$  as invariant measure, which we assume to be of the form

$$\mu(dx) = C_\mu \exp(-\Psi(x)) \prod_{i=1}^d \left( dx_i + \frac{1}{\kappa_i} \delta_0(dx_i) \right) \quad (1.2)$$

for some differentiable negated score function  $\Psi$ , normalising constant  $C_\mu > 0$  and positive parameters  $\kappa_1, \kappa_2, \dots, \kappa_d$ . Here the Dirac masses are located at 0, but generalizations are straightforward. The resulting samplers and processes are referred to as *sticky samplers* and *sticky piecewise deterministic Markov processes* respectively. The proportionality constant  $C_\mu$  is assumed to be unknown while  $(\kappa_i)_{i=1, \dots, d}$  are known. This is a natural assumption; for example, the posterior  $\mu_{\text{post}}(dx) \propto L(x)\mu_0(dx)$  appearing in Bayesian inference with spike-and-slab prior and likelihood  $L$  is equivalent to (1.2), with

$$\exp(-\Psi(x)) = L(x) \prod_{i=1}^d \pi_i(x_i) \quad (1.3)$$

and

$$w_i = \left( 1 + \frac{\pi_i(0)}{\kappa_i} \right)^{-1}, \quad i = 1, 2, \dots, d, \quad (1.4)$$

so that the prior and the likelihood imply a particular form of  $\Psi$  and  $(\kappa_i)_{i=1, \dots, d}$ .

Relevant quantities which are used for model selection, such as the posterior probability of a model without the first variable

$$\mu(\{0\} \times \mathbb{R}^{d-1}) = C_\mu \int \exp(-\Psi(x)) \frac{1}{\kappa_1} \delta_0(dx_1) \prod_{i=2}^d \left( dx_i + \frac{1}{\kappa_i} \delta_0(dx_i) \right)$$

cannot be directly computed if  $C_\mu$  is unknown. However, given a trajectory  $(x(t))_{0 \leq t \leq T}$  of the continuous time process with invariant measure  $\mu$ , the quantity  $\mu(\{0\} \times \mathbb{R}^{d-1})$  can be approximated by considering the ratio  $T_0/T$  where  $T_0 = \text{Leb}\{0 \leq t \leq T: x_1(t) = 0\}$ . This simple, yet general idea requires the user only to set  $\{\kappa_i\}_{i=1}^d$  and  $\Psi$  according to the relations given in equation (1.3) and equation (1.4). Moreover, the posterior probability that a collection of variables are all jointly equal to zero can be estimated in a similar way by computing the fraction of time that all corresponding

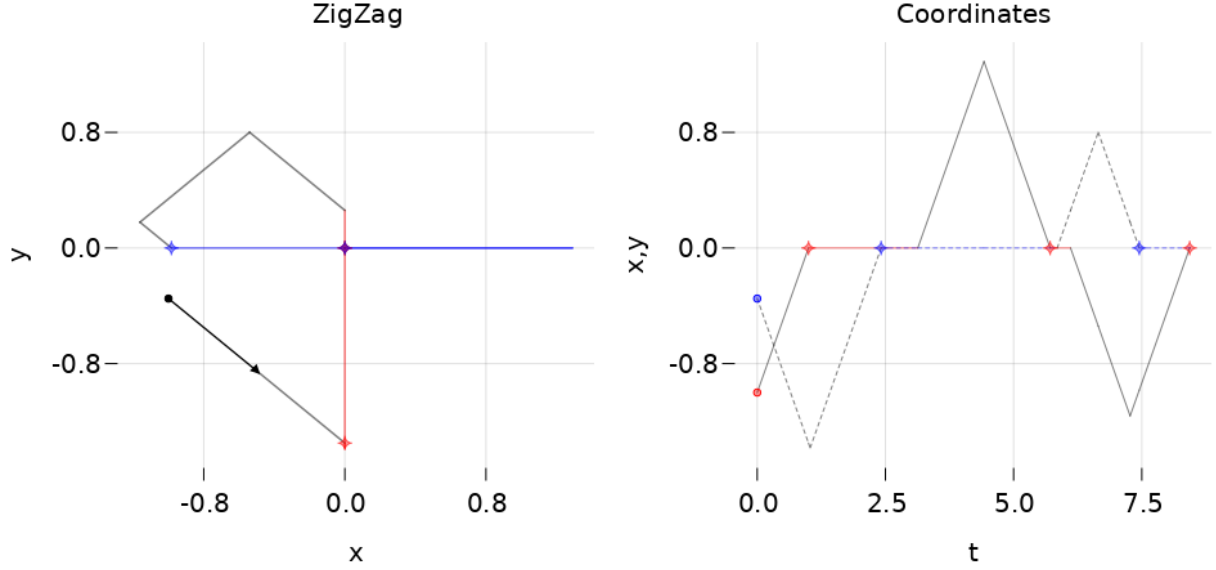


FIGURE 1: 2-dimensional sticky Zig-Zag sampler. On the left panel, a trajectory on the  $(x, y)$ -plane of the sticky Zig-Zag sampler targeting a standard normal measure. The sticky event times relative to the  $x$  (respectively  $y$ ) coordinate and the trajectories with the  $x$  (respectively  $y$ ) stuck at 0 are marked with a blue (respectively red) cross and line. On the right panel, the trajectories of each coordinate against the time using the same (color-) scheme. The trajectory of  $y$  is dashed.

coordinates of the process are simultaneously zero and, more generally, credible sets and expectations of functionals with respect to the posterior can be estimated from the simulated trajectory.

### 1.1 Related literature

Statistical inference under sparsity has received considerable attention over the past few decades. From a Bayesian perspective, the spike-and-slab prior measures create sparse posterior measures with non-zero probabilities for the coefficients to be exactly 0. As such, they are suitable for variable selection. These were firstly introduced in Mitchell and Beauchamp (1988) in the context of regression problems and afterwards used in conjunction with Markov Chain Monte Carlo methods (e.g. Ishwaran and Rao, 2005). A general and common framework for MCMC methods for variable selections was introduced in Green (1995) and Green and Hastie (2009) and referred as *reversible jump MCMC*.

We acknowledge independent and parallel work by Chevallier, Fearnhead, and Sutton (2020) which, similar to us, proposed a variable selection technique based on PDMP samplers. Our approach is different, since Chevallier, Fearnhead, and Sutton (2020) rely on the framework of reversible jumps between models which induces random walk behaviour while jumping between models, as the probability to jump from a state  $x$  in a model  $i$  to a state  $y$  in model  $j$ , with  $i \neq j$  and the probability to jump back from  $y$  to  $x$  have to satisfy the detailed balance condition.

On the contrary, the approach presented here changes model in *non-reversible* steps so that the momentum of each particle is not lost while exploring different models. The sampler has no additional tuning parameters, just the same tuning parameters as the non-sticky version of the PDMP sampler. This way we also do not require additional tuning parameters for the decision whether to move to a smaller dimensional model or not, which would have to be chosen based on empirical criteria.

### 1.2 Outline

Section 2 introduces and formalises the sticky samplers. Appendix A integrates this section with theoretically oriented results. In Section 3 we present the subsampling technique for the sticky samplers

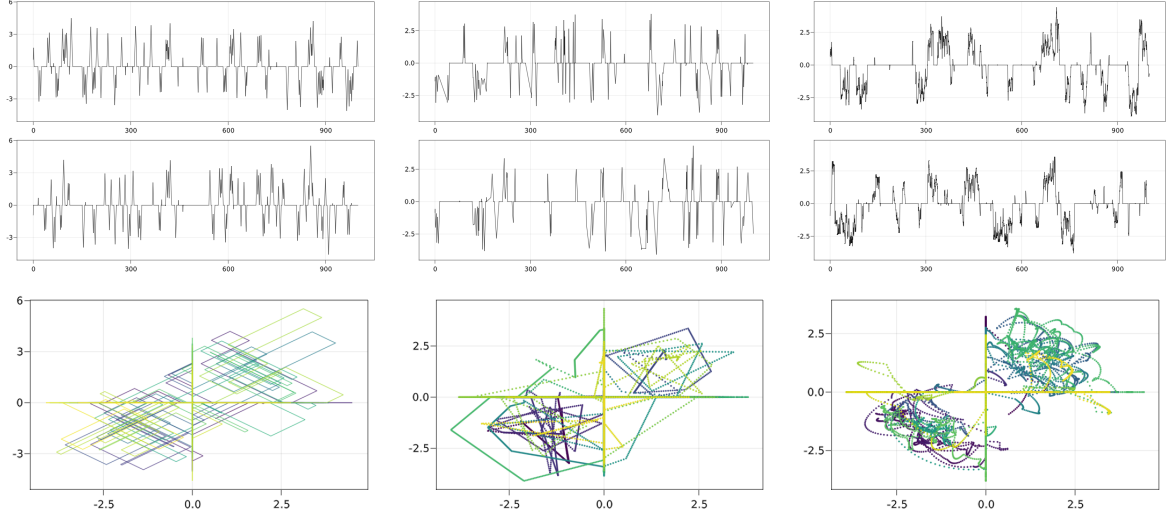


FIGURE 2: Behaviours of 3 different sticky PDMP samplers targeting a mixture of two bivariate Gaussian densities centered respectively in the first and the third quadrant of the  $x$ - $y$  axes. Top: trace plots of  $x$  and  $y$ -coordinates. Bottom: relative  $(x$ - $y$ ) phase portraits, with the time represented by colour. Left: sticky Zig-Zag sampler. Middle: sticky Bouncy Particle sampler with refreshment rate equal to 0.1. Right: sticky Boomerang sampler with refreshment rate equal to 1.0. For all the samplers,  $\kappa_1 = \kappa_2 = 0.1$  and the final clock was set to  $T = 1000$ . As the sticky Bouncy Particle sampler and the Boomerang sampler don't have constant speed, we marked their continuous trajectories in the phase plots with dots. The distance of dots indicates the speed of traversal.

and in particular for the sticky Zig-Zag sampler. In Section 4 we discuss the algorithmic implementation details of the sticky samplers and the computational efficiency of the algorithm. The Julia package (Schauer and Grazzi, 2021) implements the sticky PDMP samplers from this article for general use. In Section 5, the sticky Zig-Zag sampler is used to sample the posterior density in a number of non-trivial examples.

### 1.3 Notation

The  $i$ th element of the vector  $x \in \mathbb{R}^d$  is denoted by  $x_i$ . We denote  $x_{-i} := (x_1, x_2, \dots, x_{i-1}, x_{i+1}, \dots, x_d) \in \mathbb{R}^{d-1}$ . Write

$$(x[k:y])_i := \begin{cases} x_i & i \neq k, \\ y & i = k. \end{cases}$$

Write  $[x]_A := (x_i)_{i \in A} \in \mathbb{R}^{|A|}$  for a set of indexes  $A \subset \{1, 2, \dots, d\}$  with cardinality  $|A|$ . The inner product and the norm operator in the subspace determined by  $A$  is denoted by  $\langle x, v \rangle_A := \sum_{i \in A} x_i v_i$  and  $\|x\|_A := \sum_{i \in A} x_i^2$  with the convention that  $\langle \cdot, \cdot \rangle_{\{1, 2, \dots, d\}} = \langle \cdot, \cdot \rangle$  and  $\|\cdot\|_{\{1, 2, \dots, d\}} = \|\cdot\|$ . We denote by  $\sqcup$  the disjoint union between sets and the positive and negative part of a real-valued function  $f$  by  $f^+ := \max(0, f)$  and  $f^- := \max(0, -f)$  respectively so that  $f = f^+ + f^-$ . Denote by  $\mathcal{M}(E)$  the class of measurable functions  $f: E \rightarrow \mathbb{R}$  and let  $C(E) = \{f \in \mathcal{M}(E): f \text{ is continuous}\}$ . Let  $\mathcal{B}(E)$  be the Borel  $\sigma$ -algebra on  $E$ . For a finite set  $A$ , denote the uniform distribution on  $A$  by  $\text{Unif}(A)$ .

## 2 Sticky PDMP samplers

In this section we present the details of the sticky PDMP samplers considered here. Appendix A integrates this section with a theoretically oriented study of the sticky Zig-Zag sampler.

The  $d$ -dimensional sticky PDMP sampler has the same dynamics as the ordinary PDMP sampler, until one of the coordinates hits zero, in which case that coordinate sticks an exponentially distributed time to zero while the other coordinates continue their movement – if they are not stuck to zero themselves.

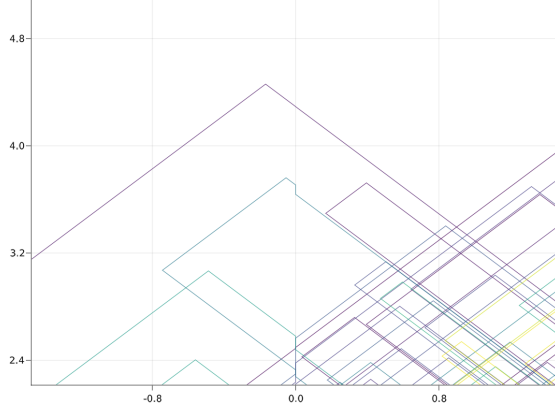


FIGURE 3: Sticky Zig-Zag (zoomed in,  $\kappa = 10$ ). Note that after sticking to the  $x$ -axis for a short time, the process continues in the previous direction, “without losing momentum”.

To preserve the Markov property, the state of the process has to contain information whether the coordinate is temporally set to zero and its value. To address this, we introduce a state space of positions and velocities, which for each coordinate position contains two copies of zero, a construction that allows a coordinate process arriving at zero from below (above) to spend an exponentially distributed time at zero before jumping to the “other” zero and continuing the dynamics: Formally, let  $\overline{\mathbb{R}}$  be the disjoint union

$$\overline{\mathbb{R}} = (-\infty, 0^-] \sqcup [0^+, \infty)$$

with the natural topology<sup>1</sup>  $\tau$ , where we use the notation  $0^-$ ,  $0^+$  to distinguish the zero element in  $(-\infty, 0]$  from the zero element in  $[0, \infty)$ .

The process will have *càdlàg*<sup>2</sup> trajectories in the locally compact state space  $E = \overline{\mathbb{R}}^d \times \mathcal{V}$ , where we will assume that either  $\mathcal{V} = \mathbb{R}^d$  (for the Bouncy particle and Boomerang samplers) or  $\mathcal{V}$  to be a finite subset of  $\mathbb{R}^d$  (in case of the Zig-Zag). Pairs of position and velocity will typically be denoted by  $(x, v) \in \overline{\mathbb{R}}^d \times \mathcal{V}$ .

A trajectory reaching zero in a coordinate from below (with positive velocity) or from above (with negative velocity) spends time at the closed end of the half open interval  $(-\infty, 0^-]$  ( $[0^+, \infty)$ ). Thus the  $i$ th coordinate of the particle is sticking to zero (or frozen), if the particle’s state is element of the  $i$ th frozen boundary  $\mathfrak{F}_i \subset E$  given by

$$\mathfrak{F}_i = \{(x, v) \in E : x_i = 0^-, v_i > 0 \text{ or } x_i = 0^+, v_i < 0\}.$$

Sometimes, we abuse notation by writing  $(x_i, v_i) \in \mathfrak{F}_i$  when  $(x, v) \in \mathfrak{F}_i$  as the set  $\mathfrak{F}_i$  has restrictions only on  $x_i, v_i$ .

The closed endpoints of the half-open intervals are somewhat reminiscent of sticky boundaries in the sense of Liggett (2010, Example 5.59). Denote by  $\alpha \equiv \alpha(x, v)$  the set of indices of active coordinates, defined by

$$\alpha = \{i \in \{1, 2, \dots, d\} : (x, v) \notin \mathfrak{F}_i\} \quad (2.1)$$

and its complement  $\alpha^C = \{1, 2, \dots, d\} \setminus \alpha$ . Furthermore define a jump or *transfer mapping*  $T_i : \mathfrak{F}_i \rightarrow E$  by

$$T_i(x, v) = \begin{cases} (x[i: 0^+], v) & \text{if } x_i = 0^-, v_i > 0, \\ (x[i: 0^-], v) & \text{if } x_i = 0^+, v_i < 0. \end{cases}$$

Sticky piecewise deterministic Markov processes on the space  $E$  are determined by their infinitesimal characteristics: their dynamics are determined by random state changes happening at random jump

<sup>1</sup>A function  $f : \overline{\mathbb{R}} \rightarrow \mathbb{R}$  is continuous if both restrictions to  $(-\infty, 0^-]$  and  $[0^+, \infty)$  are continuous. If  $f(0^-) = f(0^+)$ , we write  $f(0)$ .

<sup>2</sup>Trajectories continuous from the right, with existing limits from the left.

times of a time inhomogeneous Poisson process with intensity depending on the state of the process, and a deterministic flow governed by a differential equation in between. The state changes happen according to a Markov kernel

$$\mathcal{Q}: E \times \mathcal{B}(E) \rightarrow [0, \infty),$$

at random times sampled with state dependent intensity  $\lambda: E \rightarrow [0, \infty)$ . The deterministic dynamics are determined by the integral equation

$$(x(t), v(t)) = (x(s), v(s)) + \int_s^t \xi(x(r), v(r)) dr, \quad (2.2)$$

with  $\xi: E \rightarrow E$ , which determines the operator

$$\mathfrak{X}f = \sum_i \xi_i^x \partial_{x_i} f + \sum_i \xi_i^v \partial_{v_i} f, \quad f \in C^1(E)$$

where  $\xi^x$  and  $\xi^v$  denote the location and velocity component of  $\xi$  respectively.

Typically we think of different types of state changes given by Markov kernels  $\mathcal{Q}_1, \mathcal{Q}_2, \dots$ , for example refreshments, reflections, etc. If each transition is triggered by its individual independent Poisson clock with intensity  $\lambda_1, \lambda_2, \dots$ , then  $\lambda = \sum_i \lambda_i$ , and  $\mathcal{Q}$  itself can be written as the mixture

$$\mathcal{Q}((x, v), \cdot) = \sum_i \frac{\lambda_i((x, v))}{\lambda((x, v))} \mathcal{Q}_i((x, v), \cdot).$$

With that, the dynamics of the sticky PDMP sampler  $t \mapsto (x(t), v(t))$  are as follows: starting from  $(x, v) \in E$ ,

1. its flow in each coordinate is deterministic and continuous until an event happens. The deterministic dynamics are given by (2.2) componentwise for functions  $\xi_i: \mathbb{R} \times \mathbb{R} \rightarrow \mathbb{R} \times \mathbb{R}$  which depend on the specific PDMP chosen (typically  $\xi_i = \xi_j$  for  $i, j \in 1, \dots, d$ ). Upon hitting  $\mathfrak{F}_i$ , the  $i$ th coordinate process ceases to move (freezes), captured by the state dependence of (2.2).
2. A frozen coordinate “unfreezes” or “thaws” at rate equal to  $\kappa_i |v_i|$  by jumping according to the transfer mapping  $T_i$  to the location  $(0^+, v_i)$  respective  $(0^-, v_i)$  outside  $\mathfrak{F}_i$  and continuing with the *same* velocity as before. That is, on hitting  $\mathfrak{F}_i$ , the  $i$ th coordinate process freezes for an independent exponentially distributed time with rate  $\kappa_i |v_i|$ . This constitutes a non-reversible move between models of different dimension (see Figure 3). The corresponding transition  $\mathcal{Q}_{i, \text{thaw}}$  is the Dirac measure at  $\delta_{T_i(x, v)}$  and the intensity component  $\lambda_{i, \text{thaw}}$  equals  $\kappa_i |v_i| \mathbf{1}_{\mathfrak{F}_i}$ . This non-reversibility choice of  $\mathcal{Q}$  is the main difference between our approach and Chevallier, Fearnhead, and Sutton (2020).
3. An inhomogeneous Poisson process with rate depending on  $\Psi$  triggers the reflection events. At a reflection event time, the process changes its velocities according to its reflection rule in such a way that the process is invariant to the measure  $\mu$ .
4. Refreshment events can be added, where at exponentially distributed times the velocity (and possibly also the position) change according to a refreshment rule leaving the measure  $\mu$  invariant. Refreshments are sometimes necessary for the process to be ergodic.

A sample of the sticky PDMP is given by a recursive construction. Let  $s \rightarrow \varphi(s, x, v)$  be the deterministic solution of (2.2) starting in  $(x, v)$ , obtained by concatenating the flows solving (2.2) on the subsets of  $E$  where  $\alpha(x, v)$  is constant.

Set  $\tau_0 = 0$  and assume position and velocity vectors  $x$  and  $v$  at time 0. Given the current state  $(X(\tau_i), V(\tau_i))$  at time  $\tau_i$ , sample independently  $\Delta_i$  as the first event time of an inhomogeneous Poisson process,  $\Delta_i \sim \text{Poiss}(s \rightarrow \lambda(\varphi(s, X(\tau_i), V(\tau_i))))$ , with

$$P(\Delta_i \geq t) = \exp\left(-\int_0^t \lambda(\varphi(s, X(\tau_i), V(\tau_i))) ds\right). \quad (2.3)$$



Let  $\tau_{i+1} = \tau_i + \Delta_i$  and set for  $t \in [\tau_i, \tau_{i+1})$

$$(X(t), V(t)) = \varphi(t - \tau_i, X(\tau_i), V(\tau_i)).$$

Then let

$$(X(\tau_{i+1}), V(\tau_{i+1})) \sim \mathcal{Q}(\varphi(\Delta_i, X(\tau_i), V(\tau_i)), \cdot).$$

Then  $(X_t, V_t)$  is a sticky PDMP with dynamics  $\mathcal{Q}$ ,  $\lambda$ ,  $\varphi$ , initialised in  $(x, v)$ .

Properties of a piecewise deterministic Markov process such as a sticky sampler  $(X_t, V_t)$  with start in  $(x, v)$  can be derived from  $\mathcal{Q}$ ,  $\lambda$  and  $\mathfrak{X}$ . In particular, with the operator

$$(\mathcal{A}f)(x, v) = (\mathfrak{X}f)(x, v) + \lambda(x, v) \int (f(x', v') - f(x, v)) \mathcal{Q}((x, v), d(x', v'))$$

for all functions  $f \in \mathcal{D}(\mathcal{A})$  with

$$\mathcal{D}(\mathcal{A}) = \{f: \forall (x, v) \in E, f(X(t), V(t)) - f(x, v) + \int_0^t \mathcal{A}f(X(s), V(s)) ds \text{ are local martingales.}\}$$

as specified in Davis (1993, Section 24).

Most importantly, if  $\mu$  is such that  $\int \mathcal{A}f d\mu = 0$  for a large class of functions  $f$ , for example all  $f \in \mathcal{D}(\mathcal{A})$  and the process is Feller, then  $\mu$  is the invariant measure of the process  $(X(t), V(t))$ . Here, the operator  $\mathcal{A}$  extends the generator  $\mathcal{L}$  of the Markov process  $(X(t), V(t))$ , formally defined as

$$\mathcal{L}f(x) := \lim_{t \downarrow 0} \frac{\mathbb{E}[f(X(t), V(t)) \mid X_0 = x, V_0 = v] - f(x, v)}{t}$$

for continuous functions  $f$  for which this limit exists uniformly in  $x$  and is continuous (see Liggett, 2010, Section 3 for more details).

In what follows, we introduce the sticky version of the Zig-Zag sampler, the Bouncy Particle sampler and the Boomerang samplers. A typical realization of each of these samplers can be found in Figure 2.

## 2.1 Sticky Zig-Zag sampler

A trajectory of the sticky Zig-Zag sampler has piecewise constant velocity which is an element of the set  $\mathcal{V} = \{v: |v_i| = a_i, \forall i \in \{1, 2, \dots, d\}\}$  for a fixed vector  $a$ . For each index  $i$ , the deterministic dynamics of equation (2.2) are determined by the function  $\xi(x_i, v_i) = (v_i \mathbb{1}_{(x_i, v_i) \notin \mathfrak{S}_i}, 0)$ . Each coordinate  $(x_i, v_i)$  which is not stuck at 0 follows its dynamics until either it hits  $(0^+, -a_i) \sqcup (0^-, a_i)$  or a reflection time happens. The reflection time for the  $i$ th coordinate is determined by the inhomogeneous rate

$$\lambda_i(x, v) = \mathbb{1}_{i \in \alpha(x, v)} ((v_i \partial_i \Psi(x))^+ + \lambda_{0,i}(x)),$$

for positive functions  $\lambda_{0,i}$  which, in our experiments, we set to 0, as, in general, the smaller are the rates the more efficient is the algorithm (see for example Andrieu and Livingstone, 2019, Section 5.4). At reflection time, the sign of the velocity component of the state is flipped:  $(x_i, v_i) \rightarrow (x_i, -v_i)$ . When the coordinate hits the states  $(0^+, -a_i)$  or  $(0^-, a_i)$ , it sticks in this state for an exponentially distributed time with rate  $\kappa_i a_i$ . The formal construction of the  $d$ -dimensional sticky Zig-Zag process is rather technical and relies on the theory of piecewise deterministic processes developed in Davis (1993) (see Appendix (A) for full details). Here we highlight the main results.

Recall  $t \rightarrow \varphi(t, x, v)$  denotes the deterministic solution of (2.2) starting in  $(x, v)$  and  $\tau$  is the natural topology on  $E$  introduced in Section 2. Define the operator  $\mathcal{A}$  with domain

$$\begin{aligned} \mathcal{D}(\mathcal{A}) = \{f \in \mathcal{M}(E); t \rightarrow f(\varphi(t, x, v)) \text{ } \tau\text{-absolutely continuous } \forall (x, v); \\ \lim_{t \rightarrow 0} f(x[i: 0^+ + t], v) = f(x[i: 0^+], v); \\ \lim_{t \rightarrow 0} f(x[i: 0^- - t], v) = f(x[i: 0^-], v)\} \end{aligned}$$

by

$$\mathcal{A}f(x, v) = \sum_{i=1}^d \mathcal{A}_i f(x, v)$$

with

$$\mathcal{A}_i f(x, v) = \begin{cases} a_i \kappa_i (f(T_i(x, v)) - f(x, v)) & (x, v) \in \mathfrak{F}_i, \\ v_i \partial_{x_i} f(x, v) + \lambda_i(x, v) (f(x, v[i : -v_i]) - f(x, v)) & \text{else.} \end{cases}$$

**Proposition 2.1.** *The extended generator of the  $d$ -dimensional sticky Zig-Zag process is given by  $\mathcal{A}$  with domain  $\mathcal{D}(\mathcal{A})$ .*

*Proof.* See the Appendix A.4. □

Denote the space of compactly supported functions on  $E$  which are continuously differentiable in their first argument by  $C_c^1(E)$ . Define also  $C_b(E) = \{f \in C(E) : f \text{ is bounded}\}$  and

$$D = \{f \in C_c^1(E), \mathcal{A}f \in C_b(E)\}.$$

Our first result is that the operator  $\mathcal{A}$  restricted to  $D$  resembles the generator of the non-sticky Zig-Zag process.

**Proposition 2.2.**

$$\begin{aligned} D &= \bigcap_{i=1, \dots, d} \{f \in C_c^1(E) : v_i \kappa_i (f(T_i(x, v)) - f(x, v)) \\ &\quad = v_i \partial_{x_i} f(x, v) + \lambda_i(x, v) (f(x, v[i : -v_i]) - f(x, v)), (x, v) \in \mathcal{F}_i\}. \end{aligned}$$

For  $f \in D$ ,  $\mathcal{A}f = \mathcal{L}f$ , where  $\mathcal{L}f = \sum_{i=1}^d \mathcal{L}_i f$  with

$$\mathcal{L}_i f(x, v) = v_i \partial_{x_i} f(x, v) + \lambda_i(x, v) (f(x, v[i : -v_i]) - f(x, v)).$$

**Theorem 2.3.** *The  $d$ -dimensional sticky Zig-Zag sampler is a Feller process and a strong Markov process with unique invariant distribution*

$$\mu(dx, dv) = \frac{1}{C} \sum_{u \in \mathcal{V}} \exp(-\Psi(x)) \prod_{i=1}^d \left( dx_i + \frac{1}{\kappa_i} (\mathbb{1}_{v_i > 0} \delta_{0-}(dx_i) + \mathbb{1}_{v_i < 0} \delta_{0+}(dx_i)) \delta_u(dv) \right), \quad (2.4)$$

for some normalization constant  $C > 0$ .

*Proof.* The construction of the process and the characterization of the extended generator and its domain of the  $d$ -dimensional sticky Zig-Zag process can be found in Appendix A.1. We then prove that the process is Feller and strong Markov (Appendix A.2 and Appendix A.3). By Liggett (2010), Theorem 3.37,  $\mu$  is the unique invariant measure if, for all  $f \in D$ ,  $\int \mathcal{L}f d\mu = 0$ . This last equality is derived in Appendix A.5. □

## 2.2 Sticky Bouncy Particle sampler

The deterministic dynamics of the sticky Bouncy Particle process are identical to that of the sticky Zig-Zag process, having piecewise constant velocity. For each  $i \in \{1, 2, \dots, d\}$ , when the process hits a state  $(x, v) \in \mathfrak{F}_i$ , the  $i$ th coordinate  $(x_i, v_i)$  sticks for an exponentially distributed time with rate equal to  $\kappa_i |v_i|$  while the other coordinates continue their flow until a reflection or refreshment event happens. A reflection occurs with an inhomogeneous rate equal to

$$\lambda(x, v) = \max(0, \langle v, \nabla \Psi(x) \rangle_\alpha),$$



where  $\alpha$  is as defined in Equation (2.1). At reflection time the process jumps with a contour reflection of the active velocities with respect to  $\nabla\Psi$ :

$$(R_\Psi(x, v)v)_i = \begin{cases} v_i & i \notin \alpha(x, v) \\ v_i - 2 \frac{\langle \nabla\Psi(x), v \rangle_\alpha}{\|\nabla\Psi(x)\|_\alpha^2} \partial_i \Psi(x) & \text{else.} \end{cases}$$

Similarly to the standard Bouncy Particle sampler, the sticky Bouncy Particle sampler refreshes its velocity component at exponentially distributed times with homogeneous rate equal to  $\lambda_{\text{ref}}$ . This is necessary for avoiding pathological behaviour of the process (see Bouchard-Côté, Vollmer, and Doucet, 2015). At refreshment times, each coordinate renews its velocity component independently according to the following refreshment rule

$$v'_i \sim \begin{cases} Z_i & (x, v) \notin \mathfrak{F}_i, \\ \text{sign}(v_i)|Z_i| & (x, v) \in \mathfrak{F}_i, \end{cases} \quad (2.5)$$

where  $Z_i \stackrel{i.i.d.}{\sim} \mathcal{N}(0, 1)$ , independently of all random quantities. The refreshment rule coincides with the refreshment rule given in the standard Bouncy Particle sampler algorithm Bouchard-Côté, Vollmer, and Doucet (2015) for the coordinates whose index is in the set  $\alpha$ . For the components which are stuck at 0, the refreshment rule renews the velocity without changing its sign. This prevents the possibility for the  $i$ th stuck component to jump out the set  $\mathfrak{F}_i$  (changing its label from frozen to active at refreshment time).

The extended generator of the sticky Bouncy Particle sampler is given by

$$\mathcal{A}f(x, v) = \sum_{i=1}^d \mathcal{G}_i f(x, v) + \lambda(x, v)(f(x, R_\Psi(x, v)v) - f(x, v)) + \lambda_{\text{ref}} \int (f(x, w) - f(x, v)) \varrho_{x, v}(w) dw$$

and

$$\mathcal{G}_i f(x, v) = \begin{cases} |v_i| \kappa_i (f(T_i(x, v)) - f(x, v)) & (x, v) \in \mathfrak{F}_i \\ v_i \partial_{x_i} f(x, v) & \text{else,} \end{cases}$$

where

$$\varrho_{x, v}(w) = \rho(w_{\alpha(x, v)}) \prod_{i \in \alpha(x, v)^c} 2\rho(w_i) \mathbb{1}_{v_i w_i > 0},$$

for sufficient regular functions  $f: E \rightarrow \mathbb{R}$  in the extended domain of the generator. Here,  $\rho(y)$  is the standard normal density function evaluated at  $y$ .

**Proposition 2.4.** *The  $d$ -dimensional sticky Bouncy Particle sampler is invariant to the measure*

$$\mu(dx, dv) = \frac{1}{C} \exp(-\Psi(x)) \prod_{i=1}^d \left( dx_i + \frac{1}{\kappa_i} (\mathbb{1}_{v_i > 0} \delta_{0-}(dx_i) + \mathbb{1}_{v_i < 0} \delta_{0+}(dx_i)) \rho(v) dv \right) \quad (2.6)$$

for some normalization constant  $C$ .

*Proof.* See Appendix A.5. □

**Remark 2.5.** In more generality, the transition kernel at refreshment times can be chosen as follows: with two refreshment transition densities  $q^A$  and  $q^F$  such that  $q^A(w_A | v_A)\rho(v_A)$  and  $q^F(w_F | v_F)\rho(v_F)$  for each  $A \sqcup F = \{1, \dots, d\}$  are symmetric densities in  $w, v$ , the refreshment kernel

$$\varrho_{x, v}(dy, dw) = q^A(w_{\alpha(x, v)} | w_{\alpha(x, v)}) q^F(w_{\alpha^c(x, v)} | w_{\alpha^c(x, v)}) \delta_{\mathcal{F}(x, v, w)}(dy) dw$$

where

$$(\mathcal{F}(x, v, w))_i = \begin{cases} 0^- & \text{if } x_i = 0^+, v_i < 0, w_i > 0, \\ 0^+ & \text{if } x_i = 0^-, v_i > 0, w_i < 0, \\ x_i & \text{else} \end{cases}$$

leaves the target measure  $\mu$  invariant.

The transition kernels given in Remark 2.5 satisfy the equation  $\lambda_{\text{ref}} \int f(x, w) - x(x, v) \varrho_{x, w} dw d\mu = 0$  and therefore, by similar computations as in Appendix A.5.2, leave  $\mu$  invariant. For example, the preconditioned Crank-Nicolson scheme Cotter et al. (2013) falls within this setting.

### 2.3 Sticky Boomerang sampler

The sticky Boomerang sampler has Hamiltonian dynamics prescribed by the vector field  $\xi(x_i, v_i) = (v_i, -x_i)$  with close-form solution

$$(x_i(t), v_i(t)) = (\cos(t)x_i(0) + \sin(t)v_i(0), -x_i(0)\sin(t) + \cos(t)v_i(0)), \quad (2.7)$$

and is invariant to a prescribed Gaussian measure centered in 0. Define  $U(x)$  such that

$$U(x) = \Psi(x) - \frac{1}{2}x'\Sigma^{-1}x$$

for a positive semi-definite matrix  $\Sigma \in \mathbb{R}^{d \times d}$ . Consider for example the application in Bayesian inference with spike-and-slab prior (equation (1.1)) where  $\{\pi_i\}_{i=1}^d$  are centered Gaussian densities with variance  $\sigma_i^2$ . Then a natural choice is  $\Sigma = \text{Diag}(\sigma_1^2, \sigma_2^2, \dots, \sigma_n^2)$ .

Similarly to the sticky Bouncy Particle sampler, the process reflects its velocity at an inhomogeneous rate given by

$$\lambda(x, v) = \langle v, \nabla U(x) \rangle_\alpha^+$$

with reflection specified by the transition kernel

$$(R_U(x, v)v)_i = \begin{cases} v_i & i \notin \alpha \\ v_i - 2 \frac{\langle \nabla U(x), v \rangle_\alpha}{\|\nabla \Sigma^{1/2} U(x)\|_\alpha^2} \langle \Sigma_{[i,:]}, \nabla U(x) \rangle_\alpha & \text{else} \end{cases}$$

and refreshes the velocity at exponentially distributed times with rate equal to  $\lambda_{\text{ref}}$  according to the rule given in equation (2.5).

**Proposition 2.6.** *The  $d$ -dimensional sticky Boomerang sampler is invariant to the measure in equation (2.6).*

*Proof.* See Appendix A.5. □

A variant of the sticky Boomerang sampler is the sticky factorised Boomerang sampler (being the sticky version of the factorised Boomerang sampler introduced in Bierkens et al., 2020). Here the process has the same dynamics, refreshment rule and sticky events of the sticky Boomerang process but has a different reflection rate and reflection rule. Similarly to the sticky Zig-Zag process, the first reflection time of the sticky factorised Boomerang sampler is given by the minimum of  $|\alpha(x, v)|$  Poisson times  $\{\tau_j : j \in \alpha(x, v)\}$  with  $\tau_j \sim \text{Poiss}(t \rightarrow \lambda_j(\varphi(t, x, v)))$  and  $\lambda_j(x, v) = (\partial_{x_j} U(x)v_j)^+$ . Likewise the sticky Zig-Zag process, at the reflection time the process reflects its velocity by changing the sign of the  $i$ th component  $v \rightarrow v[i: -v_i]$  where  $i = \arg\min\{\tau_j : j \in \alpha(x, v)\}$ . As shown in Bierkens et al. (2020) and argued briefly in Section 4, the factorised Boomerang sampler can outperform the standard Boomerang sampler when  $\partial_{x_i} U$  is function of few coordinates (see Section 4 for the computational advantages of factorised samplers).

## 3 Subsampling

Here we address the problem of sampling a  $d$ -dimensional target measure when the log-likelihood is a sum of  $N$  terms, when  $d$  and  $N$  are large. Consider for example a regression problem where both the number of covariates and the number of experimental units in the dataset are large. In this situation the full evaluation of the log-likelihood and its gradient is prohibitive. However, PDMP samplers can still be used with the exact subsampling technique (e.g. Bierkens, Fearnhead, and Roberts, 2019) as this allows for substituting the gradient of the log-likelihood (which is required for deriving the reflection times) by an estimate of it which is cheaper to evaluate, without introducing any bias on the output of the sampler.

We present the exact subsampling technique for the sticky Zig-Zag sampler. Analogous subsampling techniques can be devised for the sticky Bouncy Particle sampler and the sticky Boomerang sampler as well.

The subsampling technique for sticky PDMP samplers requires to find an unbiased estimate of the gradient of  $\Psi$  in (1.2). To that end, assume the following decomposition:

$$\partial_{x_i} \Psi(x) = \left( \sum_{j=1}^{N_i} S(x, i, j) \right), \quad \forall x \in \mathbb{R}^d, i = 1, 2, \dots, d, \quad (3.1)$$

for some scalar valued function  $S$ .

For fixed  $(x, v)$  and a tuning parameter  $x^*$ , for each  $i \in \alpha(x, v)$  the random variable

$$N_i (S(x, i, J) - S(x^*, i, J)) + \partial_{x_i} \Psi(x^*), \quad J \sim \text{Unif}(\{1, 2, \dots, N_i\})$$

is an unbiased estimator for  $\partial_{x_i} \Psi(x)$ . Define the Poisson rates

$$\tilde{\lambda}_{i,j}(x, v) = (v_i N_i (S(x, i, j) - S(x^*, i, j)) + v_i \partial_{x_i} \Psi(x^*))^+$$

and, for each  $i \in \alpha$ ,  $t \geq 0$ , the bounding rates  $\bar{\lambda}_i(t, x, v) \geq \tilde{\lambda}_{i,j}(\varphi(t, x, v))$ ,  $\forall j \in \{1, 2, \dots, N_i\}$ . The sticky Zig-Zag with subsampling has the following dynamics:

- the deterministic dynamics and the sticky events are identical to the ones of the standard Zig-Zag sampler presented in Section 2.1;
- A *proposed* reflection time equals  $\min_{i \in \alpha(x, v)} \tau_i$ , with  $\{\tau_i\}_{i \in \alpha(x, v)}$  independent and  $\tau_i \sim \text{Poiss}(s \rightarrow \lambda_i(s, x, v))$ ;
- at the proposed reflection time  $\tau$  triggered by the  $i$ th Poisson clock, the process reflects its velocity according to the rule  $(x, v) \rightarrow (x, v[i, -v_i])$  with probability  $\lambda_{i,j}(\varphi(\tau, x, v)) / \bar{\lambda}_i(\tau, x, v)$  where  $J \sim \text{Unif}(\{1, 2, \dots, N_i\})$ .

We call the resulting sampler the *sticky Zig-Zag subsampler*.

**Proposition 3.1.** *The sticky Zig-Zag subsampler leaves the measure in equation (2.4) invariant.*

*Proof.* Fix  $(x, v)$ ,  $x^*$  and a proposed reflection time  $\tau > 0$  triggered by the  $i$ th coordinate with  $i \in \alpha(x, v)$ . Write  $x', v' = \varphi(\tau, x, v)$ . The probability to reflect the  $i$ th velocity at time  $\tau$  is given by

$$\mathbb{E}_J \left[ \frac{\tilde{\lambda}_{i,J}(x', v')}{\bar{\lambda}_i(\tau, x, v)} \right] = \frac{m_i(x', v')}{\bar{\lambda}_i(\tau, x, v)} \leq 1$$

with

$$m_i(x, v) = \sum_{j=1}^N (v_i (S(x, i, j) - S(x^*, i, j)) + v_i \partial_{x_i} \Psi(x^*))^+.$$

By the thinning argument for Poisson processes (e.g. Grimmett and Stirzaker, 2001), the effective reflection rate relative of the  $i$ th coordinate is  $m_i(x, v)$ . Notice that

$$m_i(x, v) - m_i(x, v[i, -v_i]) = v_i \partial_{x_i} \Psi(x), \quad i = 1, 2, \dots, d$$

and the same computations carried in Appendix A.5.1 follows with  $\lambda_i$  replaced by  $m_i$ .  $\square$

The number of computations required by the sticky subsampler to compute the next event time with respect to the quantity  $N$  is  $\mathcal{O}(1)$  (since  $\partial_{x_i} \Psi(x^*)$  can be pre-computed). This advantage comes at the cost of introducing ‘shadow event times’, which are event times where the velocity component does not reflect. The advantage of using subsamplers over the standard samplers have been empirically shown and informally argued for example in Bierkens, Fearnhead, and Roberts (2019, Section 5) and Bierkens et al. (2020, Section 3) in regimes where the Bernstein von-Mises theorem holds (large  $N$ ) and when choosing  $x^*$  to be the mode of the smooth component of the posterior density.

## 4 Simulating sticky PDMPs

### 4.1 Overview

Sticky samplers can be implemented recursively by modifying appropriately the standard PDMP samplers so to include sticky events as introduced in Section 2. In this section we show the computational benefits of having particles stuck at 0. We discuss how to integrate local implementations of the standard algorithms to increase the sampler’s performance in case of a sparse dependency structure in the target measure and in case of local upper-bounding rates.

Although PDMPs have continuous trajectories, the algorithm computes and saves only a finite collection of points (which we refer to as the skeleton of the continuous trajectory) corresponding to the positions, velocities and times where the deterministic dynamics of the process change. In between those points, the continuous trajectory can be deterministically interpolated.

In case the  $i$ th partial derivative of the negative score function is a sum of  $N_i$  terms, which is the case for example in regression problems, subsampling techniques can be employed as described in Section 3.

### 4.2 Computing Poisson times for PDMPs

As PDMPs move deterministically (and with simple dynamics) in between event times, the main computational challenge consists of simulating those times. Given an initial position  $(x, v)$ , the distribution of the time until the next event is specified in (2.3). A sample from this distribution can be found by solving for  $t$  in the equation

$$\int_0^t \lambda(\varphi(s, x, v)) ds = \tau', \quad \tau' = \text{Exp}(1). \quad (4.1)$$

We then write that  $\tau' \sim \text{Poiss}(s \rightarrow \lambda(\varphi(s, x, v)))$ . When it is not possible to find the root of equation (4.1) in closed form, it suffices to find upper bounds  $\bar{\lambda}$  for the rate functions which satisfies, for any  $(x, v) \in S$  and  $t \geq 0$ ,

$$\bar{\lambda}(t, x, v) \geq \lambda(\varphi(t, x, v)),$$

and for which this is possible and use the thinning scheme. The simulation of sticky times is easier: once the  $i$ -th component hits zero then it sticks at zero for a time that is exponentially distributed with parameter  $\kappa_i |v_i|$ .

For the standard  $d$ -dimensional Zig-Zag and the factorised Boomerang sampler (these samplers are called *factorised PDMPs* in Bierkens et al., 2020), the reflection time is factorised as the minimum of  $d$  independent clocks and (4.1) splits up in  $d$  equations  $\int_0^t \lambda_i(\varphi(s, x, v)) ds = \tau'_i$ ,  $\tau'_i \stackrel{\text{i.i.d.}}{=} \text{Exp}(1)$ , for  $i = 1, 2, \dots, d$ .

The first reflection time of the  $d$ -dimensional sticky factorised samplers is obtained instead by finding the minimum of  $|\alpha| < d$  independent clocks with the same rates  $\lambda_i$  of the standard factorised sampler, but only for the active coordinates  $i \in \alpha(x, v)$ .

Here, it is clear that having many particles stuck at 0 is advantageous, since the number of computations is of order  $\mathcal{O}(|\alpha|)$  with  $|\alpha| \ll d$ . This is to be contrasted to the  $d$ -dimensional standard factorised sampler, for which the order of computation is always  $\mathcal{O}(d)$ .

If  $\partial_{x_i} \Psi$  (an estimate of  $\partial_{x_i} \Psi$  when using subsampling) or the upper bound  $\bar{\lambda}$  depend on fewer coordinates, then the evaluation of each reflection time is cheaper. The fully local implementation presented in Bierkens et al. (2020) exploits these two features once in proposing the reflection time and once for deciding whether to accept.

We discuss in more details the sticky Zig-Zag sampler with local upper-bounds and with subsampling.

### 4.3 The local sticky Zig-Zag

#### 4.3.1 Local implementation

Assume that the sets  $\bar{A}_i$  and  $\bar{\lambda}_i$  are such that

$$\bar{\lambda}_i(t, x, v) = f_i(t, x_{\bar{A}_i}), \quad \forall x, \text{ for } i = 1, 2, \dots, d$$

for some  $f_i: \mathbb{R}^+ \times \mathbb{R}^{|\bar{A}_i|} \rightarrow \mathbb{R}^+$  with  $\bar{A}_i \subset \{1, 2, \dots, d\}$ . Given an initial position  $(x, v)$  and random times  $\tau_j \sim \text{Pois}(t \rightarrow \bar{\lambda}_j(t, x, v))$ , for  $i \in \alpha$ , denote by  $i = \arg\min_{j \in \alpha(x, v)}(\tau_j)$  and  $\tau = \min_{j \in \alpha(x, v)}(\tau_j)$  the first proposed reflection time. According to the thinning procedure for Poisson processes, the process flips the  $i$ th coordinate with probability  $\lambda_i(\varphi(\tau, x, v))/\bar{\lambda}_i(\tau, x, v)$ . If the process flips the  $i$ th velocity, then the Poisson rates  $\{\bar{\lambda}_j: j \in \alpha, \bar{A}_j \not\ni i\}$  continue to be valid upper bounds so that the corresponding reflection times do not need to be renewed (see Bierkens et al., 2020, Section 4, for implementation details).

In general, when the  $i$ th particle freezes at 0 or was stuck at 0 and gets released, the reflection times  $\tau_j: i \in \bar{A}_j$  have to be renewed. However this is not always the case, as there are applications, such as the one in Section 5.1, for which the upper-bounding rates  $\{\bar{\lambda}_i\}_{i=1}^d$  continue to be valid upper bounds when one or more particles hit 0 and therefore the waiting times computed before the particles hit 0 are still valid.

#### 4.3.2 Fully local implementation

Consider now the decomposition of  $\partial_{x_i}\Psi$ ,  $i = 1, 2, \dots, d$  given in equation (3.1) and such that

$$S(x, i, j) = f_{i,j}(x_{\tilde{A}_{i,j}}), \quad \forall x, \text{ for } (i, j) \in \{1, 2, \dots, d\} \times \{1, 2, \dots, N_i\}$$

for some  $f_{i,j}: \mathbb{R}^{|\tilde{A}_{i,j}|} \rightarrow \mathbb{R}$  with  $\tilde{A}_{i,j} \subset \{1, 2, \dots, d\}$ .

The fully local implementation of the sticky Zig-Zag subsampler profits from local upper bounds and local gradient estimators by assigning an independent time for each coordinate, thus evolving the flow of only the coordinates which are required at each step and by stacking all the reflection times  $\tau_j: j \in \alpha$ , the hitting times  $\tau_j^*: j \in \alpha$  and the unfreezing times  $\tau_j^\circ: j \in \alpha^c$  in an ordered queue. For a documented implementation, see Schauer and Grazzi (2021).

Given an initial point  $(x, v)$  and if  $i$  is the coordinate of the first proposed reflection time  $\tau_i = \min(\tau_j: j \in \alpha(x, v))$ , the sampler reflects the velocity of the  $i$ th coordinate with probability  $\tilde{\lambda}_{i,J}(x_{\tilde{A}_i}(t), v)/\bar{\lambda}(t, x, v)$  with  $J \sim \text{Unif}(\{1, 2, \dots, N_i\})$ . Hence, it is only required to update the position of the coordinates with index in  $\tilde{A}_{i,J} \setminus \alpha^C(x, v)$ . Then,

- if the  $i$ th velocity flips, then the algorithm needs to update only the waiting times  $\{\tau_j: j \in \alpha, \bar{A}_j \ni i\}$  (as described in Subsection 4.3.1) and, to this end, needs to update the position of the coordinates with index  $\{k \in \bar{A}_j \setminus \alpha^c(x, v): i \in \bar{A}_j\}$ ;
- in the other case, when the  $i$ th velocity does not change (shadow event), only  $\tau_i$  has to be renewed so that only the particles in  $\bar{A}_i$  have to be updated.

## 5 Examples

In this section we apply sticky and non-sticky PDMP samplers and subsamplers to three different problems:

- a sparse logistic regression model where we assume both the number of covariates ( $d$ ) and the sample size ( $N$ ) to be large and the coefficient vector to be sparse;
- an image (given as  $n \times n$ -matrix  $X$ ) which is black outside a region of interest is observed with white noise;

- a  $p$ -dimensional stochastic differential equation where the drift is given as sparse, unknown linear map  $X \in \mathbb{R}^{p \times p}$  is observed continuously.

Hence, in the first case the vector of regression coefficients is the parameter of the model, where in the second and the third case it is the matrix  $X$ . In all cases we simulate data from the model and assume the parameter to be sparse (i.e. most of its elements are zero) and high dimensional. As we understand, the high dimensionality of the parameter space considered here (e.g. 10,000) exceeds the scope of other available Bayesian variable selection methods. As a benchmark for comparisons, Appendix C contains detailed results obtained when running the sticky Zig-Zag sampler in a challenging scenario of high dimensional parameter space.

We focus on the Zig-Zag process, which does not require refreshment events and has simple factorised dynamics which allows for a local implementation, although the other sticky samplers are available in Schauer and Grazzi (2021) for these examples as well. For the logistic regression we compare the sticky Zig-Zag subsampler with the standard Zig-Zag subsampler, while for the other two examples we compare the sticky Zig-Zag sampler with the standard Zig-Zag sampler. In each case, the sticky version targets a measure of the form of equation (1.2) while the standard (sub)sampler targets the measure proportional to  $\exp(-\Psi(dx))$  (which corresponds to the sticky Zig-Zag sampler with  $\kappa_1 = \kappa_2 = \dots = \kappa_d = \infty$ ). In each case we compare functionals of the posterior measure estimated by trajectories of equal length given by the output of the samplers.

All the simulations are carried out on an ordinary laptop computer and can be easily reproduced using the code available at <http://github.com/mschauer/ZigZagBoomerang.jl/research/sticky> within minutes. Considering problem sizes or parameter dimensions and additional difficulties such as correlated parameters or non-linearities as in the logistic regression problem clearly establish the competitiveness of our method (and implementation).

## 5.1 Logistic regression

Suppose  $\{0, 1\} \ni Y_i \mid x \sim \text{Ber}(\psi(x^T a_i))$  with  $\psi(u) = (1 + e^{-u})^{-1}$ .  $a_i \in \mathbb{R}^d$  denotes a vector of covariates and  $x \in \mathbb{R}^d$  a parameter vector. Assume  $Y_1, \dots, Y_N$  are independent, conditional on  $x$ . Let the design matrix  $A \in \mathbb{R}^{N \times p}$  be the matrix where the  $i$ -th row is the vector  $a_i$ . We assume a spike-and-slab prior of (1.1), assuming  $\pi_1 = \pi_2 = \dots = \pi_d$  to be zero mean Gaussian densities with some (large) variance  $\sigma^2$ . This implies that the posterior measure is of the form of equation (1.2) with

$$\Psi(x) = \sum_{j=1}^N \left( \log \left( 1 + e^{\langle A_{[j,:], x} \rangle} \right) - y_j \langle A_{[j,:], x} \rangle \right) + \frac{1}{2\sigma^2} \|x\|^2$$

and  $\kappa_1, \kappa_2, \dots, \kappa_d$  as in (1.4).

We consider two categorical features with 21 levels each and two continuous features. Each case is independently assigned a random level of each discrete feature and a random value of the continuous features,  $N(0, 0.1^2)$ . Our design matrix  $A$  then includes the levels of the discrete features in dummy encoding (40 columns) and the interaction terms between them also in dummy encoding scaled by 0.3 (400 columns), and the continuous features in the final two columns ( $d = 442$ ). We then generate  $N = 35360$  observations using as ground truth a sparse coefficient vector  $x$  with 10% fill-in.

We run the sticky ZigZag subsampler and the standard subsampler with bounding rates derived in Appendix B. We choose  $w_1 = w_2 = \dots = w_d = 0.9$  (the proportion of non-zero elements of parameter vector  $x$ ) and  $\sigma^2 = 100$ . The implementation makes use of a sparse matrix representation of  $A$ , speeding up the computation of inner products  $\langle A_{[j,:], x} \rangle$ .

With this setting, we observe that the sticky Zig-Zag algorithm is approximately 10 times faster than the standard Zig-Zag algorithm. Figure 4 shows the discrepancy between the parameters used during simulation and the estimated posterior median relative to the two samplers. The sum of absolute errors is 55 and 417 respective for the sticky Zig-Zag sampler and Zig-Zag sampler. Table 1 shows the confusion matrix relative to the posterior median for the sticky Zig-Zag sampler, and the confusion matrix of estimate of the standard sampler using a threshold to identify zeros. The threshold was

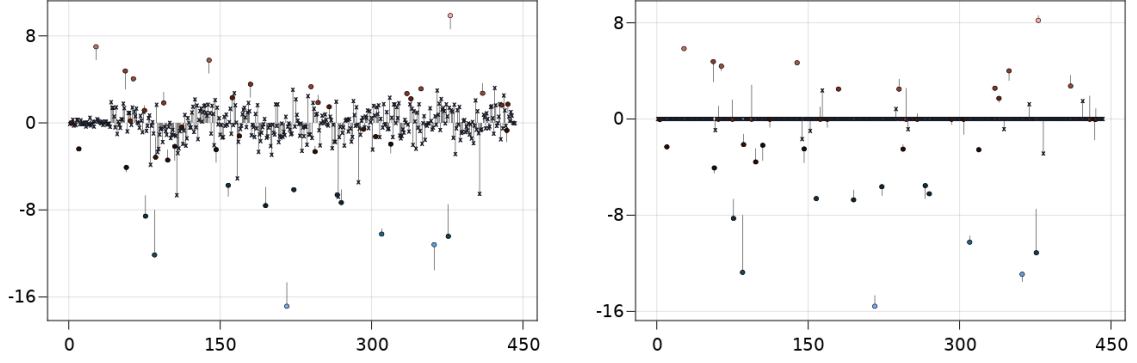


FIGURE 4: Posterior median estimate of logistic regression coefficients, sticky Zig-Zag with spike-and-slab prior on the right, corresponding Gaussian model (with  $\kappa_i = \inf$  for all  $i$ ) on the left. Thin vertical lines indicate distance to the truth. True zeros are plotted with the symbol  $\times$ , other are plotted as points with color gradient corresponding to the ground truth.

	<i>Thresholding</i>		<i>Sticky Zig-Zag</i>	
	Predicted		Predicted	
	non-zero	zero	non-zero	zero
True non-zero	11	33	11	33
True zero	65	333	9	389

TABLE 1: Confusion matrix (Sparse logistic regression).

chosen such that the first row of the confusion matrices of the estimate with threshold and the sticky Zig-Zag sampler match.

## 5.2 Spatially structured sparsity

We consider the problem of inference on a spatially correlated and sparse signal. The signal is an  $n \times n$  image, represented by  $x \in \mathbb{R}^d$ ,  $d = n^2$ . We view  $x$  as a vector but use both linear indexing  $x_k$  and Cartesian indexing  $x_{i,j}$  to refer to the component at index  $k = n(i-1) + j$ . Assume  $x$  is observed corrupted with white noise

$$Y_{i,j} = x_{i,j} + Z_{i,j}, \quad Z_{i,j} \stackrel{\text{i.i.d.}}{\sim} \mathcal{N}(0, \sigma^2), \quad i, j \in \{1, \dots, n\}.$$

Assume that  $x \equiv 0$  outside a region of interest (ROI). The negative log-likelihood is of the form of  $\ell(x) = C + \frac{\|x - Y\|^2}{2\sigma^2}$  for some constant  $C > 0$  which does not depend on  $x$ .

A quadratic negative log-density

$$\Psi_0(x) = \frac{1}{2} x' \Gamma x$$

(which would give rise to a Gaussian measure with respect to a Lebesgue reference measure) is likewise meaningful as unnormalised density with respect to the product of mixtures of Lebesgue and Dirac measures

$$\lambda(dx) = \prod_{i=1}^d \left( dx_i + \frac{1}{\kappa} \delta_0(dx_i) \right). \quad (5.1)$$

This means that similar to the situation in the Gaussian case where a Gaussian prior is conjugate for this model, if the prior has quadratic negative logarithmic density with respect to the spike-and-slab



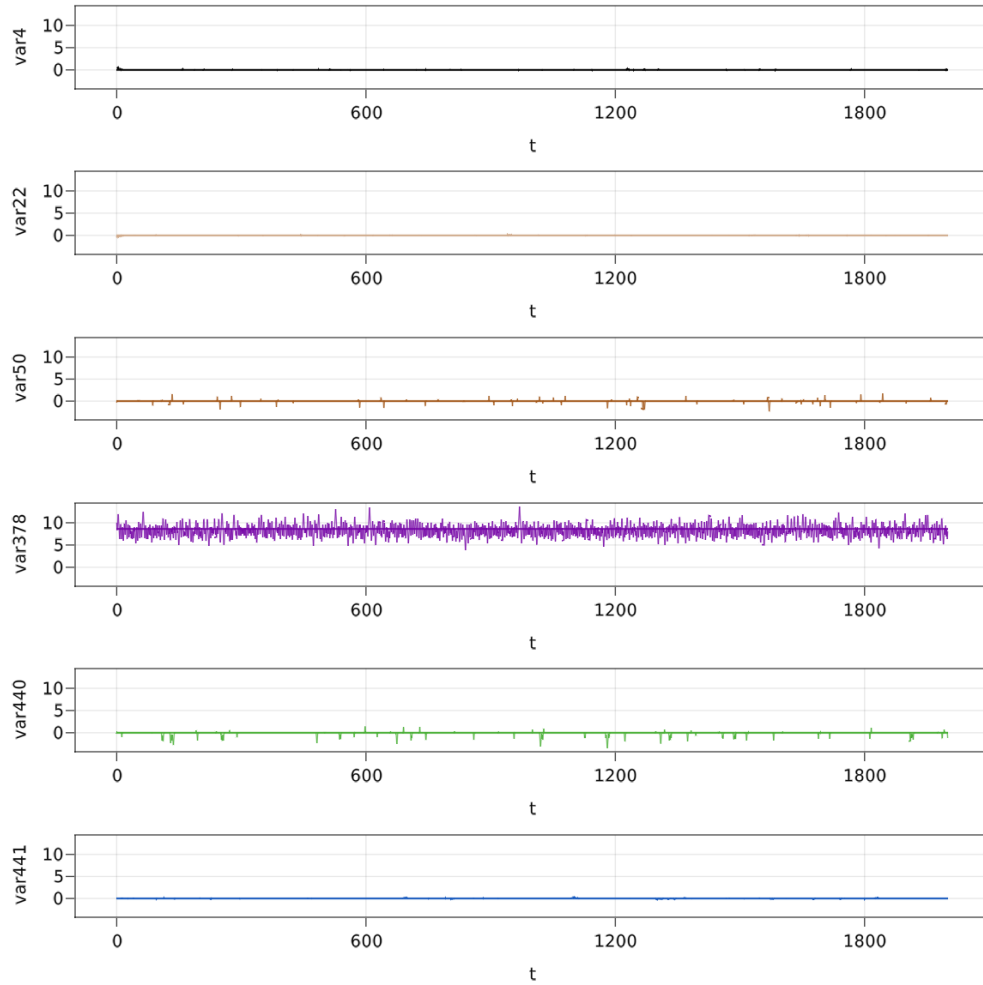


FIGURE 5: Trace plots of selected coefficients for the sparse logistic regression. The trajectories which explore areas around 0 spend most of their time stuck at 0. A constant line indicates the true value of the coefficients when different from 0.

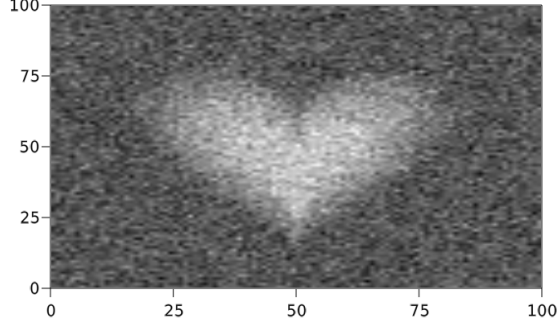


FIGURE 6: An image observed with white noise. Outside the region of interest (heart shape), the true image is black (0).

measure (5.1), then the negative logarithmic posterior density with respect to (5.1) is quadratic as well. This is numerically convenient, see below.

The Gaussian mixture component of the prior  $\mu_0(dx) = \Psi_0(x)\lambda(dx)$  and  $\{\kappa_i\}_{i=1,\dots,d}$  can be chosen to encourage smoothness, sparsity and local clustering of zero entries and non-zero entries.

For example one can take  $\Gamma$  to be the precision matrix of the Gaussian density  $\Psi_0$  corresponding to a  $L_2$  penalty on the local differences. Here we choose  $\Gamma = c\Lambda$  where  $\Lambda$  is the graph Laplacian of the pixel neighbourhood graph, defined as in Mider, Schauer, and Meulen (2020, Section 7.3): the pixel indices  $i, j$  are identified with the vertices  $V = \{(i, j), i \in \{1, \dots, n\}, j \in \{1, \dots, n\}\}$  of the  $n \times n$ -lattice with edges  $E = \{\{v, v'\} : v = (i, j), v' = (i', j') \in V, |i - i'| + |j - j'| = 1\}$  (using the set notation for edges). Thus, edges connect a pixel to its vertical and horizontal neighbours. Then

$$\lambda_{v,v'} = \begin{cases} \text{degree}(v) & v = v' \\ -1 & \{v, v'\} \in E \\ 0 & \text{otherwise} \end{cases}$$

and

$$\Lambda = (\Lambda_{kl})_{k,l \in \{1, \dots, n^2\}} \quad \text{with} \quad \Lambda_{(i-1)n+j, (k-1)n+l} = \lambda_{(i,j), (k,l)}, \quad \text{for} \quad i, j, k, l \in \{1, \dots, n\}.$$

This prior is applicable in similar situations such as the fused Lasso in Tibshirani et al. (2005). This is different to for example Gugushvili, Shota et al. (2019) which encourages small and large values to cluster respectively, but makes no prior assumption on positive or negative correlation of neighboring pixels.

We assume that pixel  $(i, j)$  corresponds to a physical location of size  $\Delta u_1 \times \Delta u_2$  centered at  $u(i, j) = u_0 + (i\Delta u_1, j\Delta u_2) \in \mathbb{R}^2$ .

To numerically illustrate our approach, we use a heart shaped region given by

$$x_{i,j} = 5 \max(1 - h(u(i, j)), 0)$$

where  $h: [-1.5, 1.5] \times [-1.1, 1.9] \rightarrow [0, \infty)$  is defined by

$$h(u) = u_1^2 + \left( \frac{5u_2}{4} - \sqrt{|u_1|} \right)^2$$

and  $u_0 = (-1.5, -1.1)$ ,  $\Delta u_1 = \Delta u_2 = \dots$ ,  $n = 200$ .

In the example, about 80% of the pixels of the truth are black, but we emphasize that this example can represent a small region of a much larger otherwise black picture.

Figure 6 shows the observation  $Y$ . We run the sticky Zig-Zag sampler as explained above with  $\Psi(x) = \ell(x)\Psi_0(x)$  and choose the smoothing prior parameters  $\kappa_1 = \kappa_2 = \dots = \kappa_d = 0.4$ . Then,  $\Psi$  is

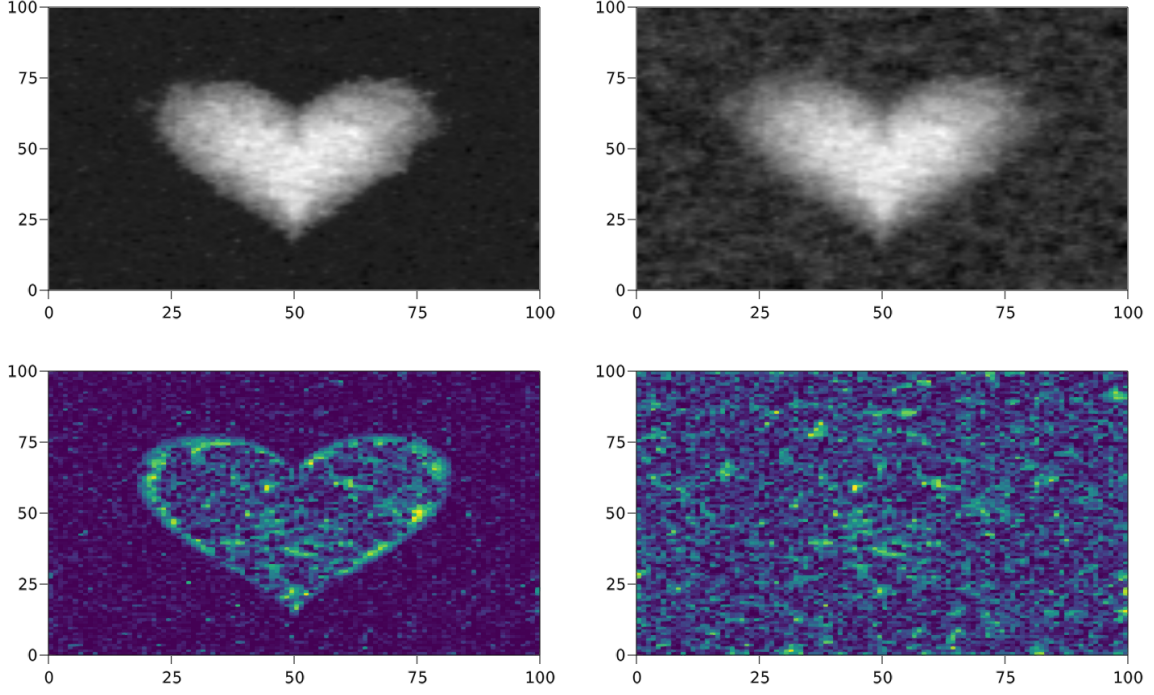


FIGURE 7: Heart shaped example of spatially structured sparsity. Left: sticky Zig-Zag sampler with spike-and-slab prior. Right: Gaussian smoother (corresponding to  $\kappa = \infty$ ). Top: posterior mean; bottom: Error of the mean estimate, with the same color scale on both images.

quadratic for  $x$  (equal to a Gaussian log-density up to additive constants) and the reflection times of the sticky Zig-Zag sampler can be computed in closed form without thinning schemes. Figure 7 shows the estimated posterior mean of the signal (left) and its deviation from the true signal  $x$ . By applying the sticky Zig-Zag over the standard Zig-Zag sampler we can reduce for example the error by a factor of 2 (see the bottom panels in Figure 7) and the computational time by a factor of 10.

### 5.3 Learning networks of stochastic differential equations

Consider the linear, multivariate  $p$ -dimensional Itô stochastic differential equation

$$dY_t = XY_t dt + \sigma dW_t, \quad Y_0 = y_0, \quad t \in [0, T]. \quad (5.2)$$

Here  $W$  is a  $p$ -dimensional Wiener process,  $X \in \mathbb{R}^{p \times p}$  is a square matrix determining the dynamics of  $Y$ , and  $\sigma$  is a positive scalar dispersion constant. The task is to estimate  $X$  from observation of a trajectory of  $Y$  on the interval  $[0, T]$ . We assume  $X$  is sparse, and the non-zero entries  $x_{i,j}$  of  $X$  encode a directed relationship between coordinates  $Y_i$  and  $Y_j$ . See Bento, Ibrahimi, and Montanari (2010) and references therein for similar set-ups. Determining  $X$  from the observation  $(Y_t)_{0 \leq t \leq T}$  gives rise to a sparse regression problem.

Following Reynolds (1987) and in the presentation JuliaCon 2020 with Jesse Bettencourt (2020), we consider a process  $Y$  taking values in  $\mathbb{R}^{2p}$ , where each pair  $(y_{2i-1}, y_{2i})$  is the location of an autonomously moving agent (a “boid”) in 2-dimensional space and  $X$  is defined by its action on vectors by

$$Xy = -\lambda y + \sum_{i=1}^p \sum_{1 \leq j \leq d} \theta_{ij} \phi_{ij}(y),$$

where  $(\theta_{ij})$  is a sparse matrix encoding relationship between agents and (using linear indices)

$$\phi_{ij}(x) = (x_{2j-1} - x_{2i-1})e_{2i-1} + (x_{2j} - x_{2i})e_{2i},$$

where  $e_i$  is the standard basis in  $\mathbb{R}^{2p}$ . We assume  $\theta_{ii} = 0$  as  $\phi_{ii} \equiv 0$  for  $i \in \{1, \dots, d\}$ .

	<i>Thresholding</i>		<i>Sticky Zig-Zag</i>	
	Predicted		Predicted	
	non-zero	zero	non-zero	zero
True non-zero	83	17	83	17
True zero	154	2246	25	2375

TABLE 2: Confusion matrix (Network SDE)

The dynamics encode that each boid can be repelled or attracted by another boid. If  $\theta_{ij} > 0$ , agent  $i$  with location  $y_{2i-1,2i}$  has the tendency to follow agent  $j$ ; if  $\theta_{ij} < 0$ ,  $i$  tends to avoid  $j$ . See Grazzi and Schauer (2021) for a small animation of the trajectories of the agents in time.

From standard results in stochastic differential equations, the likelihood of  $X$  given the process  $(Y_t)$  written with respect to the law of the standard  $d$ -dimensional Wiener process is given by Girsanov’s formula:

$$\exp \left( \frac{1}{\sigma^2} \int_0^T (XY_t)' dY_t - \frac{1}{2\sigma^2} \int_0^T \|XY_t\|^2 dt \right).$$

Completing the square, this implies that the negated log-likelihood of  $\theta$  (written as vector in column order) takes the form

$$\ell(\theta) = C + \frac{1}{2}(\theta - \mu)' \Gamma (\theta - \mu)$$

for some  $C$ , where  $\mu = \Gamma^{-1}z$  with

$$z = \sigma^2 \int_0^T \Phi(Y_s)' (1 - \lambda) dY_s$$

and

$$\Gamma = \sigma^2 \int_0^T \Phi(Y_s)' \Phi(Y_s) ds.$$

Here,  $\Phi(y)$  is the matrix having column vectors  $\phi_{i,j}(y) \in \mathbb{R}^{p^2}$  for  $i, j \in \{1 \leq i, j \leq d: i \neq j\}$  (see Mider, Schauer, and Meulen, 2020, Section 5.2).

With this parametrization of  $X$ , we are interested in inference for  $\theta \in \mathbb{R}^d$  with  $d = p^2 - p$ . Unlike Section 5.2, here we choose a product form prior for  $\theta$  as in equation (1.1). This is appropriate if  $p$  is large and  $X$  is sparse. The task is then to sample (1.2) with  $\Psi$  as in (1.3). Thus we choose  $\pi_1 = \pi_2 = \dots = \pi_d$  to be Gaussian measures with some large variance  $\sigma_0^2$  and  $\kappa_1 = \kappa_2 = \dots = \kappa_d$  as in (1.4). With this choice,  $\Psi$  is quadratic for  $\theta$  and, similarly to the spatially structured sparsity example, the reflection times of the sticky Zig-Zag sampler can be computed in closed form.

We set  $p = 50$ ,  $T = 200$ ,  $\sigma = 0.1$  and simulate  $(Y_t)_{0 \leq t \leq T}$  according to the model in equation (5.2) forward in time with the Euler discretization scheme, with small step size equal to 0.1.  $w_1 = w_2 = \dots = w_d$  is chosen to be the proportion of non-zero elements of parameter  $\theta$  from which  $Y$  was simulated.  $\sigma_0^2 = 50$ . Figure 8 shows the discrepancy between the parameters used during simulation and the estimated posterior median relative to the two samplers. The sum of absolute errors and the computational time are approximately 20 times smaller for the sticky Zig-Zag sampler compared to the Zig-Zag sampler. Table 2 shows the confusion matrix using the posterior median for the sticky Zig-Zag sampler. The confusion matrix of the standard sampler is obtained by finding the threshold so to match the first row of the confusion matrix found with the sticky Zig-Zag sampler.

## Acknowledgement

This work is part of the research programme *Bayesian inference for high dimensional processes* with project number 613.009.034c, which is (partly) financed by the Dutch Research Council (NWO) under

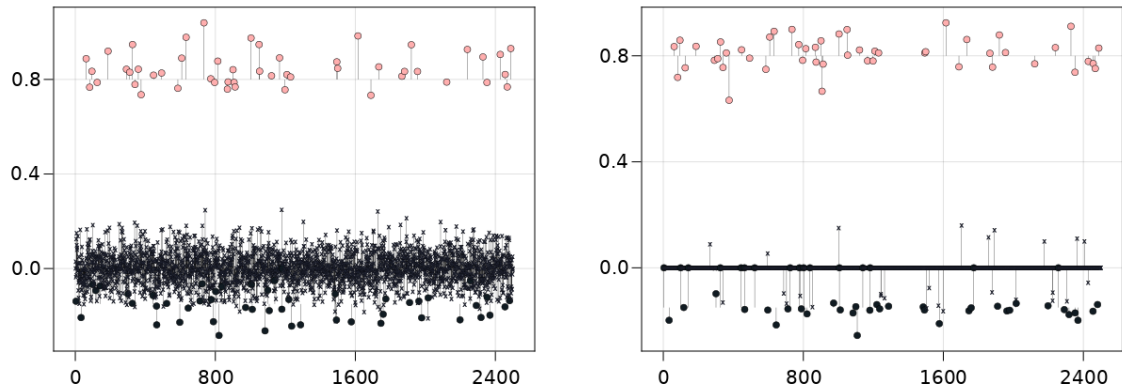


FIGURE 8: Posterior median estimate of boid interaction parameters. Sticky Zig-Zag with spike-and-slab prior on the right, corresponding Gaussian model (with  $\kappa_i = \infty$  for all  $i$ ) on the left. Thin vertical lines indicate distance to the truth. True zero coefficient are plotted with the symbol  $\times$ , other coefficients are plotted as points with color gradient corresponding to the ground truth.

the *Stochastics – Theoretical and Applied Research* (STAR) grant. J. Bierkens acknowledges support by the NWO for the research project *Zig-zagging through computational barriers* with project number 016.Vidi.189.043.

## References

- [1] Christophe Andrieu and Samuel Livingstone. *Peskun-Tierney ordering for Markov chain and process Monte Carlo: beyond the reversible scenario*. 2019. arXiv: 1906.06197.
- [2] José Bento, Morteza Ibrahimi, and Andrea Montanari. *Learning Networks of Stochastic Differential Equations*. 2010. arXiv: 1011.0415.
- [3] Joris Bierkens, Paul Fearnhead, and Gareth Roberts. “The Zig-Zag process and super-efficient sampling for Bayesian analysis of big data”. In: *Ann. Statist.* 47.3 (June 2019), pp. 1288–1320.
- [4] Joris Bierkens et al. “A piecewise deterministic Monte Carlo method for diffusion bridges”. In: *arXiv e-prints*, arXiv:2001.05889 (Jan. 2020). arXiv: 2001.05889.
- [5] Joris Bierkens et al. *The Boomerang Sampler*. 2020. arXiv: 2006.13777.
- [6] Alexandre Bouchard-Côté, Sebastian J. Vollmer, and Arnaud Doucet. “The Bouncy Particle Sampler: A Non-Reversible Rejection-Free Markov Chain Monte Carlo Method”. In: *arXiv e-prints*, arXiv:1510.02451 (2015). arXiv: 1510.02451.
- [7] Augustin Chevallier, Paul Fearnhead, and Matthew Sutton. *Reversible Jump PDMP Samplers for Variable Selection*. 2020. arXiv: 2010.11771.
- [8] Nicolas Chopin and James Ridgway. *Leave Pima Indians alone: binary regression as a benchmark for Bayesian computation*. 2015. arXiv: 1506.08640.
- [9] Simon L. Cotter et al. “MCMC methods for functions: modifying old algorithms to make them faster”. In: *Statistical Science* (2013), pp. 424–446.
- [10] M. H. A. Davis. *Markov models and optimization*. Vol. 49. Monographs on Statistics and Applied Probability. Chapman & Hall, London, 1993, pp. xiv+295. ISBN: 0-412-31410-X.
- [11] Simon Duane et al. “Hybrid Monte Carlo”. In: *Physics letters B* 195.2 (1987), pp. 216–222.
- [12] Sebastiano Grazi and Moritz Schauer. *Boid animation*. <https://youtu.be/01VoURPwVLI>. Youtube, 2021. URL: <https://youtu.be/01VoURPwVLI>.
- [13] Peter J. Green. “Reversible jump Markov chain Monte Carlo computation and Bayesian model determination”. In: *Biometrika* (1995), p. 16.

- [14] Peter J Green and David I Hastie. “Reversible jump MCMC”. In: *Genetics* 155.3 (2009), pp. 1391–1403.
- [15] Geoffrey Grimmett and David Stirzaker. *Probability and random processes*. Oxford University Press, 2001.
- [16] Gugushvili, Shota et al. “Bayesian wavelet de-noising with the Caravan prior”. In: *ESAIM: PS* 23 (2019), pp. 947–978.
- [17] Hemant Ishwaran and J. Sunil Rao. “Spike and slab variable selection: Frequentist and Bayesian strategies”. In: *The Annals of Statistics* 33.2 (2005), 730–773. ISSN: 0090-5364.
- [18] JuliaCon 2020 with Jesse Bettencourt. “*JuliaCon 2020 — Boids: Dancing with Friends and Enemies*”. 2020. URL: <https://www.youtube.com/watch?v=8gS6wejsGsY>.
- [19] Thomas M Liggett. *Continuous time Markov processes*. Vol. 113. Graduate Studies in Mathematics. American Mathematical Society, Providence, RI, 2010.
- [20] Marcin Mider, Moritz Schauer, and Frank van der Meulen. *Continuous-discrete smoothing of diffusions*. 2020. arXiv: 1712.03807.
- [21] Toby J Mitchell and John J Beauchamp. “Bayesian variable selection in linear regression”. In: *Journal of the American Statistical Association* 83.404 (1988), pp. 1023–1032.
- [22] Craig W. Reynolds. “Flocks, Herds and Schools: A Distributed Behavioral Model”. In: *Association for Computing Machinery*, 1987.
- [23] L.C.G. Rogers and D. Williams. *Diffusions, Markov Processes, and Martingales: Volume 1, Foundations*. Cambridge Mathematical Library. Cambridge University Press, 2000.
- [24] Moritz Schauer and Sebastiano Grazi. *mschauer/ZigZagBoomerang.jl: v0.6.0*. Version v0.6.0. Mar. 2021. URL: <https://doi.org/10.5281/zenodo.4601534>.
- [25] Robert Tibshirani et al. “Sparsity and smoothness via the fused lasso”. In: *Journal of the Royal Statistical Society: Series B (Statistical Methodology)* 67.1 (2005), pp. 91–108.

## A Detailed study of the sticky Zig-Zag

In this section, we closely follow the general construction of piecewise deterministic processes and the main results of Davis (1993, Section 24). In order to facilitate the reading of the section, we follow the same notation of Davis (1993) so that the results derived here can be compared easily.

### A.1 Construction

In this section we discuss how the sticky Zig-Zag can be constructed as a *standard* PDMP in the sense of Davis (1993). The construction is a bit tedious, but the underlying idea is simple: the sticky Zig-Zag process has the dynamics of a standard Zig-Zag process until it reaches a freezing boundary  $\mathfrak{F}_i = \{(x, v) \in E : x_i = 0^-, v_i > 0 \text{ or } x_i = 0^+, v_i < 0\}$  of  $E = \mathbb{R}^d \times \mathcal{V}$ , with  $\mathbb{R} = (-\infty, 0^-] \sqcup [0^+, \infty)$  which has two copies of 0. Then it immediately changes dynamics and evolves as a lower dimensional standard Zig-Zag process *on the boundary*, at least until an unfreezing event happens or upon reaching yet another freezing boundary in the domain of the restricted process.

Davis' construction allows a standard PDMP to make instantaneous jumps at boundaries of open sets, but puts restrictions on further behaviour at that boundary. We circumvent these restrictions by first splitting up the space  $\mathbb{R}^d \times \mathcal{V}$  into disconnected components in a way somewhat different than the construction of  $E$  as presented in Section 2. Only at a later stage we recover the definition of  $E$ .

Define the set

$$K = \{\rightarrow \circ, \circ \rightarrow, \leftarrow \circ, \circ \leftarrow, \overset{\leftarrow}{\circ}, \overset{\rightarrow}{\circ}\}$$

and

$$|K| = \{\circ, \leftarrow \circ \rightarrow, \rightarrow \circ \leftarrow\}$$

(note that  $|K|$  does not denote the cardinality of the set  $K$ ). Define the functions  $k: \mathbb{R} \times \mathbb{R} \rightarrow K$  and  $|k|: \mathbb{R} \times \mathbb{R} \rightarrow |K|$  by

$(x, v)$	$k(x, v)$	at $(x, v)$ the process is...	$ k (x, v)$
$x > 0, v > 0$	$\circ \rightarrow$	...moving away from 0 with positive velocity	$\leftarrow \circ \rightarrow$
$x < 0, v < 0$	$\leftarrow \circ$	...moving away from 0 with negative velocity	$\leftarrow \circ \rightarrow$
$x > 0, v < 0$	$\circ \leftarrow$	...moving toward 0 with negative velocity	$\rightarrow \circ \leftarrow$
$x < 0, v > 0$	$\rightarrow \circ$	...moving toward 0 with positive velocity	$\rightarrow \circ \leftarrow$
$x = 0, v > 0$	$\overset{\rightarrow}{\circ}$	...at 0 with positive velocity	$\circ$
$x = 0, v < 0$	$\overset{\leftarrow}{\circ}$	...at 0 with negative velocity	$\circ$

If  $(x, v) \in \mathbb{R}^d \times \mathcal{V}$ , then extend  $k: \mathbb{R}^d \times \mathcal{V} \rightarrow K^d$  and  $|k|: \mathbb{R}^d \times \mathcal{V} \rightarrow |K|^d$  by applying the map  $k$  and  $|k|$  coordinatewise.

For each  $\ell \in K^d$  define

$$\tilde{E}_\ell^\circ = \{(\ell, x, v) : k(x, v) = \ell\}$$

Note that for  $\ell \neq \ell'$  the sets  $\tilde{E}_\ell^\circ$  and  $\tilde{E}_{\ell'}^\circ$  are disjoint. The set  $\tilde{E}_\ell^\circ$  is open under the metric introduced in Davis (1993), p.58, which sets the distance between two points  $(\ell, x, v)$  and  $(\ell', x', v')$  to 1 if  $\ell \neq \ell'$ . We denote the induced topology on  $\tilde{E}$  by  $\tilde{\tau}$ .  $\tilde{E}_\ell^\circ$  is a subset of  $\mathbb{R}^{2d}$  of dimension  $d_\ell = \sum_{i=1}^d \mathbb{1}_{|\ell_i| \neq \circ}$ , since the velocities are constant in  $\tilde{E}_\ell^\circ$  and the position of the components  $i$  where  $\ell_i = \circ$  are constant as well in  $\tilde{E}_\ell^\circ$  ( $\tilde{E}_\ell^\circ$  is isomorphic to an open subset of  $\mathbb{R}^{d_\ell}$ ).

The sets which contain a singleton, i.e.  $|\tilde{E}_\ell^\circ| = 1$ , are those sets  $\tilde{E}_\ell^\circ$  such that  $|\ell_i(x, v)| = \circ$  for all  $i = 1, 2, \dots, d$  and are open as they contain one isolated point, but will have to be treated a bit differently. Then  $\tilde{E}^\circ = \bigcup_{\ell \in K^d} \tilde{E}_\ell^\circ$  is the tagged space of open subsets of  $\mathbb{R}^{d_\ell}$  used in Davis (1993, Section 24).

$\tilde{E}^\circ$  separates the space into isolated components of varying dimension. In each component, the sticky Zig-Zag process behaves differently and essentially as a lower dimensional Zig-Zag process.



Let  $\partial\tilde{E}_\ell^\circ$  denote the boundary of  $\tilde{E}_\ell^\circ$  in the embedding space  $\mathbb{R}^{d_\ell}$  (where the velocity components are constant in  $\tilde{E}_\ell^\circ$ ), with elements written  $(\ell, x, v)$ . Some points in  $\partial\tilde{E}_\ell^\circ$  will also belong to the state space  $\tilde{E}$  of the sticky Zig-Zag process, but only the entrance-non-exit boundary points:

$$\tilde{E} = \bigcup_{\ell} \tilde{E}_\ell, \quad \tilde{E}_\ell = \tilde{E}_\ell^\circ \cup \{(\ell, x, v) \in \partial\tilde{E}_\ell^\circ : x_i = 0 \Rightarrow |\ell_i| \neq \circ \leftarrow \text{ for all } i\}.$$

(This corresponds to the definition of the state space in Davis (1993, Section 24), only that we use knowledge of the flow.)

The remaining part of the boundary is

$$\Gamma = \bigcup_{\ell} \Gamma_\ell \subset \bigcup_{\ell} \partial\tilde{E}_\ell^\circ, \quad \Gamma_\ell = \{(\ell, x, v) \in \partial\tilde{E}_\ell^\circ, \exists i : x_i = 0, |\ell_i| = \circ \rightarrow\},$$

with  $\tilde{E} \cap \Gamma = \emptyset$  so that  $\Gamma$  is not part of the state space  $\tilde{E}$ . Any trajectory approaching  $\Gamma$ , jumps back into  $\tilde{E}$  just before hitting  $\Gamma$ . If  $\tilde{E}_\ell^\circ$  is a singleton ( $|\tilde{E}_\ell^\circ| = 1$ ), then  $\Gamma_\ell = \emptyset$  and  $\tilde{E}_\ell = \tilde{E}_\ell^\circ$  (atoms).

**Lemma A.1.** *A bijection  $\iota : \tilde{E} \rightarrow E$  is given by*

$$\iota((\ell, \tilde{x}, v)) = (x, v)$$

where

$$x_i = \begin{cases} 0^+ (0^-) & \ell_i = \circ \leftarrow (\ell_i = \circ \rightarrow) \\ 0^+ (0^-) & \ell_i = \circ \rightarrow (\ell_i = \leftarrow \circ), \tilde{x}_i = 0 \\ \tilde{x}_i & \text{otherwise.} \end{cases}$$

*Proof.* Recall that  $\alpha(x, v) := \{i \in \{1, 2, \dots, d\} : (x, v) \notin \mathfrak{F}_i\}$  and  $\alpha^c$  denotes its complement. First of all, notice that  $\iota(\tilde{E}) \subset E$ . Now let  $(x, v) \in E$  be given. We construct  $e \in \tilde{E}$  such that  $(x, v) = \iota(e)$ . If there is at least one  $x_j = 0^\pm$  with  $j \notin \alpha(x, v)$ , then take  $e = (\ell, \tilde{x}, v) \in \tilde{E} \setminus \tilde{E}^\circ$  as follows (entrance-non-exit boundary): for  $i \in \alpha^c$  we have  $|\ell_i| = \circ$ ,  $\tilde{x}_i = 0$ , while for all  $i \in \alpha$  with  $x_i = 0^\pm$ , we have  $|\ell_i| = \leftarrow \circ \rightarrow$ ,  $\tilde{x}_i = 0$ . Then  $\iota(e) = (x, v)$ . Otherwise,  $e = (k(\tilde{x}, v), \tilde{x}, v) \in \tilde{E}^\circ$  (interior of an open set) and  $\iota(e) = (x, v)$  where  $\tilde{x}_i = 0$  for all  $i \in \alpha(x, v)$  and  $\tilde{x}_i = x_i$  otherwise.  $\square$

Having constructed the state space, we proceed with the process dynamics. Firstly, the deterministic flow (locally Lipschitz for every  $\ell \in K$ ) is determined by the functions  $\tilde{\phi}_\ell : [0, \infty) \times \tilde{E}_\ell^\circ \rightarrow \tilde{E}_\ell^\circ$  which for the sticky ZigZag process are given by

$$\tilde{\phi}(t, \ell, x, v) = (\ell, x', v), \quad \forall (\ell, x, v) \in E,$$

with  $x_i + v_i t (\mathbb{1}_{|\ell_i| \neq \circ})$ ,  $i = 1, 2, \dots, d$  and determines the vector fields

$$\mathfrak{X}_\ell \tilde{f}(\ell, x, v) = \sum_{i=1}^d \mathbb{1}_{|\ell_i| \neq \circ} v_i \partial_{x_i} f(\ell, x, v), \quad f \in C^1(\tilde{E}).$$

Sometimes we write  $\tilde{\phi}_k(t, x, v) = \tilde{\phi}(t, k, x, v)$  for convenience. Next, further state changes of the process are instantaneous, deterministic jumps from the boundary  $\Gamma$  into  $\tilde{E}$

$$\mathcal{Q}^f(((\ell, x, v), \cdot)) = \delta_{(k(x, v), x, v)}, \quad (\ell, x, v) \in \Gamma$$

and random jumps at random times corresponding to unfreezing events

$$\mathcal{Q}^s((\ell, x, v), \cdot) = \frac{\sum_i \lambda_i^s(\ell, x, v) \delta_{(\ell[i : \ell'_i], x, v)}}{\sum_i \lambda_i^s(i, x, v)}$$

with  $\ell'_i = \circ \rightarrow$  if  $\ell_i = \vec{\circ}$  and  $\ell'_i = \circ \leftarrow$  if  $\ell_i = \overleftarrow{\circ}$ , and random reflections

$$\mathcal{Q}^r((\ell, x, v), \cdot) = \frac{\sum_i \lambda_i^r(\ell, x, v) \delta_x \delta_{v[i: -v_i]} \delta_\ell}{\sum_i \lambda_i^r(\ell, x, v)}$$

with

$$\lambda_i^s(\ell, x, v) = \mathbb{1}_{|\ell_i|=\circ} \kappa_i$$

and

$$\lambda_i^r(\ell, x, v) = \mathbb{1}_{\ell_i \neq \circ} \left( (v_i \partial_i \Psi(x))^+ + \lambda_{0,i}(x) \right), \quad i = 1, 2, \dots, d.$$

Then  $\lambda: \tilde{E} \rightarrow \mathbb{R}^+$

$$\lambda(\ell, x, v) = \sum_{i=1}^d \lambda_i^r(\ell, x, v) + \lambda_i^s(i, x, v)$$

and a Markov kernel  $\mathcal{Q}: (\tilde{E} \cup \Gamma, \mathcal{B}(\tilde{E} \cup \Gamma)) \rightarrow [0, 1]$  by

$$\mathcal{Q}((\ell, x, v), \cdot) = \begin{cases} \frac{\sum_i \lambda_i^r(\ell, x, v)}{\lambda(\ell, x, v)} \mathcal{Q}^r((\ell, x, v), \cdot) + \frac{\sum_i \lambda_i^s(\ell, x, v)}{\lambda(\ell, x, v)} \mathcal{Q}^s((\ell, x, v), \cdot) & (\ell, x, v) \in \tilde{E}, \\ \mathcal{Q}^f((\ell, x, v), \cdot) & (\ell, x, v) \in \Gamma. \end{cases}$$

**Proposition A.2.**  $\mathfrak{X}, \lambda, \mathcal{Q}$  satisfy the standard conditions given in Davis (1993, Section 24.8), namely

- For each  $\ell \in K$ ,  $\mathfrak{X}_\ell$  is a locally Lipschitz continuous vector field and determines the deterministic flow  $\tilde{\phi}_\ell: \tilde{E}_\ell \rightarrow \tilde{E}_\ell$  of the PDMP.
- $\lambda: \tilde{E} \rightarrow \mathbb{R}^+$  is measurable and such that  $t \rightarrow \lambda(\tilde{\phi}_\ell(t, x, v))$  is integrable on  $[0, \varepsilon(\ell, x, v))$ , for some  $\varepsilon > 0$ , for each  $\ell, x, v$ .
- $\mathcal{Q}: \tilde{E} \cup \Gamma \rightarrow \mathcal{P}(\tilde{E})$  is measurable and such that  $\mathcal{Q}(\{(\ell, x, v)\}, (\ell, x, v)) = 0$
- The expected number of events up to time  $t$ , starting at  $(\ell, x, v)$  is finite for each  $t > 0, \forall (\ell, x, v) \in \tilde{E}$

To see the latter, remember that for any initial point  $(\ell, x, v) \in \tilde{E}$ , the deterministic flow (without any random event) hits  $\Gamma$  at most  $d$  times before reaching the singleton  $(0, 0, \dots, 0)$  and being constant there.

## A.2 Strong Markov property

**Proposition A.3.** (Part of Theorem 2.3) Let  $(\tilde{Z}_t)$  be a Zig-Zag process on  $\tilde{E}$  with characteristics  $\mathfrak{X}, \lambda, \mathcal{Q}$ . Then  $Z_t = \iota(\tilde{Z}_t)$  is a strong Markov process.

*Proof.* By Davis (1993), Theorem 26.14, the domain of the extended generator of the process  $(\tilde{Z}_t)$  with characteristics  $\mathfrak{X}, \lambda, \mathcal{Q}$  is

$$\begin{aligned} \mathcal{D}(\tilde{\mathcal{A}}) = \{f \in \mathcal{M}(\tilde{E}); t \rightarrow f(\tilde{\phi}_\ell(t, x, v)) \text{ } \tilde{\tau}\text{-absolutely continuous } \forall (\ell, x, v) \in \tilde{E}, t = [0, t_\Gamma(\ell, x, v)); \\ f(\ell, x, v) = f(\kappa(x, v), x, v), \quad (\ell, x, v) \in \Gamma\}, \end{aligned}$$

with

$$t_\Gamma(\ell, x, v) = \inf\{0 \leq t: \tilde{\phi}_\ell(t, x, v) \in \tilde{\Gamma}\}$$

and

$$\tilde{\mathcal{A}}f(\ell, x, v) = \mathfrak{X}_\ell f(\ell, x, v) + \lambda(\ell, x, v) \int_{\tilde{E}} (f(\ell', x', v') - f(\ell, x, v)) \mathcal{Q}(\ell, x, v, d(\ell, x, v)).$$

The strong Markov property of  $(\tilde{Z}_t)$  follows by Davis (1993), Theorem 25.5. Denote by  $(\tilde{P}_t)_{t \geq 0}$  the Markov transition semigroup of  $(\tilde{Z}_t)$  and let  $(P_t)_{t \geq 0}$  be a family of probability kernels on  $E$  and such that for any bounded measurable function  $f: E \rightarrow \mathbb{R}$  and any  $t \geq 0$ ,

$$\tilde{P}_t(f \circ \iota) = (P_t f) \circ \iota.$$

Then  $(P_t)_{t \geq 0}$  is the Markov transition semigroup of the process  $Z_t = (\iota(\tilde{Z}_t))$ . By Rogers and Williams (2000), Lemma 14.1, and since any stopping time for the filtration of  $(\tilde{Z}_t)$  is a stopping time for the filtration of  $(Z_t)$ ,  $Z_t$  is a *strong* Markov process.  $\square$

### A.3 Feller property

Given an initial point  $\ell, x, v \in \tilde{E}$ , let

$$t_{\Gamma_1}(\ell, x, v) = \inf\{0 \leq t: \tilde{\phi}_\ell(t, x, v) \in \tilde{\Gamma}\}$$

and define the *extended deterministic flow*  $\tilde{\varphi}: \tilde{E} \rightarrow \tilde{E}$  by setting  $\varphi(0, \ell, x, v) = (\ell, x, v)$  and recursively by

$$\tilde{\varphi}(t, \ell, x, v) = \begin{cases} \tilde{\varphi}_\ell(t, x, v) & t < t_{\Gamma_1}, \\ \tilde{\varphi}(t - t_{\Gamma_1}, k(x', v'), x', v') & t \geq t_{\Gamma_1} \end{cases}$$

with  $(\ell', x', v') = \lim_{t \rightarrow t_{\Gamma_1}} \tilde{\varphi}_\ell(t, x, v) \in \tilde{E}$ .

Observe that  $t \rightarrow \iota(\tilde{\varphi}(t, \ell, x, v))$  is continuous on  $(E, \tau)$ . Define also

$$\Lambda(t, \ell, x, v) = \int_0^t \lambda(\tilde{\varphi}(s, \ell, x, v)) ds.$$

Notice that, while  $(\ell, x, v) \rightarrow \lambda(\ell, x, v)$  has discontinuities at the boundaries  $\Gamma$ ,  $(\ell, x, v) \rightarrow \Lambda(\ell, x, v)$  is continuous. Denote by  $T_1$  the first random event (so excluding the deterministic jumps). Then for functions  $f \in B(\tilde{E})$  and  $\psi \in B(\mathbb{R}^+ \times \tilde{E})$ , set  $z(t) = (\ell(t), x(t), v(t))$  and define

$$\tilde{G}\psi(t, \ell, x, v) = E[f(z(t))\mathbb{1}_{t < T_1} + \psi(t - T_1, z(t))\mathbb{1}_{t \geq T_1}].$$

We have that

$$\tilde{G}\psi(t, \ell, x, v) = f(\tilde{\varphi}(t, \ell, x, v)) \times \mathcal{T} \quad (\text{A.1})$$

with

$$\mathcal{T} = \sum_i \int_0^t \mathbf{1}_{t \in [t_i^\Gamma, t_{i+1}^\Gamma)} \int_{x', v'} \psi(t - s, \ell, x, v) \mathcal{Q}((\ell, dx', dv'), \tilde{\varphi}(s, \ell, x, v)) \lambda(\tilde{\varphi}(s, \ell, x, v)) e^{-\Lambda(s, \ell, x, v)} ds.$$

The Feller property holds if, for each fixed  $t$  and for  $f \in C_b(E)$ , we have that  $(x, v) \rightarrow P_t f(x, v)$  is continuous (and bounded follows easily). This is what we are going to prove below, by making a detour in the space  $\tilde{E}$ , using the bijection  $\iota$  and adapting some results found in Davis (1993, Section 27), for the process  $\tilde{Z}_t$ .

**Theorem A.4.** (Part of Theorem 2.3)  $Z_t$  is a Feller process.

*Proof.* Take  $f \in C_b(\tilde{E})$  such that  $f \circ \iota \in C_b(E)$ . Call those functions on  $\tilde{E}$   $\tau$ -continuous. We want to show that  $\tilde{P}$  preserves  $\tau$ -continuity. Notice that  $\tau$ -continuous functions on  $\tilde{E}$  are such that

$$\lim_{t \rightarrow t_\Gamma} f(\tilde{\varphi}(t, \ell, x, v)) = f(\tilde{\varphi}(t_\Gamma, \ell, x, v)), \quad (\ell, x, v) \in \tilde{E}.$$

For  $\tau$ -continuous functions  $f$  and for a fixed  $t$ , the first term on the right hand side of (A.1)  $(\ell, x, v) \rightarrow f(\tilde{\varphi}(t, \ell, x, v))$  is clearly continuous. Also the second term is continuous since is of the form of an integral of a piecewise continuous function. Therefore, for any  $t \geq 0$ ,  $\psi(t, \cdot) \in B(\tilde{E})$  and  $\tau$ -continuous function  $f$ , we have that  $(\ell, x, v) \rightarrow \tilde{G}\psi(t, \ell, x, v)$  is continuous. Clearly, the (similar) operator

$$\tilde{G}_n \psi_\ell(t, x, v) = E_x[f(\tilde{\varphi}_\ell(t, x, v))\mathbb{1}_{t < T_n} + \psi(t - T_n, \tilde{\varphi}_\ell(t, x, v))\mathbb{1}_{t \geq T_n}],$$

with  $T_n$  denoting the  $n$ th random time, is continuous as well for any fixed  $n, t$ ,  $\psi(t, \cdot) \in B(\tilde{E})$  and  $\tau$ -continuous function  $f$ . By applying Lemma 27.3 in Davis (1993) we have that for any  $\psi(t, \cdot) \in B(\tilde{E})$

$$|\tilde{G}_n \psi_\ell(t, x, v) - \tilde{P}_t f(x, v)| \leq 2 \max(\|\psi\| \|f\|) P(t \geq T_n).$$

Finally, if  $\lambda$  is bounded, then we can bound  $P(t \geq T_n)$  by something which does not depend on  $(\ell, x, v)$  and goes to 0 as  $n \rightarrow \infty$  so that  $\tilde{G}_n \psi \rightarrow \tilde{P}_t f$  uniformly on  $\ell, x, v \in \tilde{E}$  under the supremum norm. This shows that, for any  $t$ ,  $\tilde{P}_t$  (and therefore  $P_t$ ) preserves  $\tau$ -continuity.  $\square$

#### A.4 The extended generator of $Z_t$

Let  $f \in \mathcal{D}(\mathcal{A})$  if  $\tilde{f} \in \mathcal{D}(\tilde{\mathcal{A}})$  and  $f \circ \iota = \tilde{f}$ . Then  $f \in \mathcal{D}(\mathcal{A})$  are  $\tau$ -absolutely continuous functions along full deterministic trajectories on  $E$ :

$$\begin{aligned} \mathcal{D}(\mathcal{A}) = \{ & f \in \mathcal{M}(E); t \rightarrow f(\varphi(t, x, v)) \text{ } \tau\text{-absolutely continuous } \forall (x, v); \\ & \lim_{t \rightarrow 0} f(x[i: 0^+ + t], v) = f(x[i: 0^+], v); \\ & \lim_{t \rightarrow 0} f(x[i: 0^- - t], v) = f(x[i: 0^-], v) \}. \end{aligned}$$

For those functions  $f \in \mathcal{D}(\mathcal{A})$  with  $f \circ \iota = \tilde{f}$  we have that

$$\tilde{\mathcal{A}}\tilde{f}(\ell, \tilde{x}, v) = \mathcal{A}f(x, v) = \sum_{i=1}^N \mathcal{A}_i f(x, v)$$

with

$$\mathcal{A}_i f(x, v) = \begin{cases} \kappa_i(f(T_i(x, v)) - f(x, v)) & (x, v) \in \mathfrak{F}_i, \\ v_i \partial_{x_i} f(x, v) + \lambda_i(x, v)(f(x, v[i: -v_i]) - f(x, v)), & \text{otherwise,} \end{cases}$$

and

$$\lambda_i(x, v) = (v_i \partial_i \Psi(x))^+ + \lambda_{0,i}(x), \quad i = 1, 2, \dots, d,$$

for positive functions  $\lambda_{0,i}$ .

**Proposition A.5.** (Proposition 2.1) *The extended generator of the process  $(Z(t))$  is given by  $\mathcal{A}$  with domain  $\mathcal{D}(\mathcal{A})$ .*

*Proof.* This is to verify that if  $f \in \mathcal{D}(\tilde{\mathcal{A}})$  and  $\tilde{\mathcal{A}}$  solve the martingale problem, i.e are such that

$$f(\ell(t), x(t), v(t)) - f(\ell, x, v) + \int_0^t \mathcal{A}f(\ell(s), x(s), v(s)) ds, \quad \forall (\ell, x, v) \in \tilde{E}$$

is a local martingale (Davis, 1993, Section 24) on  $\tilde{E}$ , then  $f \circ \iota: f \in \mathcal{D}(\tilde{\mathcal{A}})$  and  $\mathcal{A}$  solve the martingale problem on  $E$  (for any local martingale  $Z_t$  on  $\tilde{E}$ ,  $\iota(Z_t)$  is a local martingale on  $E$ ).  $\square$

By the Feller property, the extended generator is an extension of the generator defined as

$$\mathcal{L}f(x) := \lim_{t \downarrow 0} \frac{\mathbb{E}[f(X_t, V_t) \mid X_0 = x, V_0 = v] - f(x, v)}{t}$$

for a sufficient regular class of functions  $f$  for which this limit exists uniformly in  $x$  (see Liggett, 2010, Section 3, for more details). Then,  $D = \{f \in \mathcal{D}(\mathcal{A}): f \in C_b^1, \mathcal{A}f \in C_b(E)\}$  is a core for  $\mathcal{A}$  (as in Liggett, 2010, Definition 3.31). Let  $\mathcal{L}$  be the restriction of  $\mathcal{A}$  on  $D$ . By Liggett (2010, Theorem 3.37),  $\mu$  is the unique invariant measure if, for all  $f \in D$ :

$$\int \mathcal{L}f d\mu = 0.$$

#### A.5 Remaining proofs of Section 2

##### A.5.1 Invariant measure of the sticky Zig-Zag process

We check here that the sticky  $d$ -dimensional Zig-Zag process as presented in Section 2.1 taking values in  $E$  with discrete velocities in  $\mathcal{V} = \{v: |v_i| = a_i, \forall i \in \{1, 2, \dots, d\}\}$  and with extended generator  $\mathcal{A}$  is such that

$$\int \mathcal{L}f(x, v) \mu(dx, dv) = 0$$

for all  $f \in D = \{f \in C_c^1(E), \mathcal{A}f \in C_b(E)\}$ . Here,  $\mathcal{L}$  is the extended generator  $\mathcal{A}$  restricted to  $D$  (See Proposition (2.2)).

For any  $f \in D$ , define  $\lambda_i^+ := \lambda_i(x, v[i: , a_i])$ ,  $\lambda_i^- := \lambda_i(x, v[i: , -a_i])$ ,  $f_i^+ := f(x, v[i: a_i])$ ,  $f_i^- := f(x, v[i: -a_i])$ ,  $f_i^+(y) := f(x[i: y], v[i: a_i])$ ,  $f_i^-(y) := f(x[i: y], v[i: -a_i])$ . Also write the measure  $\rho(dx_i, v_i) := dx_i + \frac{1}{\kappa} (\mathbb{1}_{v_i < 0} \delta_0^+(dx_i) + \mathbb{1}_{v_i > 0} \delta_0^-(dx_i))$ . We see that

$$\begin{aligned} \int \mathcal{L}_i f d\mu = & \sum_{v \in \mathcal{V}^{-i}} \left( \int_{\mathbb{R}^{d-1}} \left( \int_{0^+}^{\infty} + \int_{-\infty}^{0^-} \right) (a_i \partial_{x_i} f_i^+ + \lambda_i^+ (f_i^- - f_i^+)) \exp(-\Psi(x)) dx_i \prod_{j \neq i} \rho(dx_j, v_j) \right) \\ & + \sum_{v \in \mathcal{V}^{-i}} \left( \int_{\mathbb{R}^{d-1}} \left( \int_{0^+}^{\infty} + \int_{-\infty}^{0^-} \right) (-a_i \partial_{x_i} f_i^- + \lambda_i^- (f_i^+ - f_i^-)) \exp(-\Psi(x)) dx_i \prod_{j \neq i} \rho(dx_j, v_j) \right) \\ & + \sum_{v \in \mathcal{V}^{-i}} \left( \int_{\mathbb{R}^{d-1}} a_i (f_i^+(0^+) - f_i^+(0^-)) \exp(-\Psi(x[i: 0])) \prod_{j \neq i} \rho(dx_j, v_j) \right) \\ & + \sum_{v \in \mathcal{V}^{-i}} \left( \int_{\mathbb{R}^{d-1}} -a_i (f_i^-(0^-) - f_i^-(0^+)) \exp(-\Psi(x[i: 0])) \prod_{j \neq i} \rho(dx_j, v_j) \right). \end{aligned}$$

By integration by parts we have that  $\left( \int_{0^+}^{\infty} + \int_{-\infty}^{0^-} \right) (\partial_{x_i} f(x, v) \exp(-\Psi(x))) dx_i$  is equal to

$$(f(x[i: 0^-], v) - f(x[i: 0^+], v)) \exp(-\Psi(x[i: 0])) + \left( \int_{0^+}^{\infty} + \int_{-\infty}^{0^-} \right) (\partial_i \Psi(x) f(x, v) \exp(-\Psi(x))) dx_i$$

so that  $\int \mathcal{L}_i f d\mu$  is equal to

$$\begin{aligned} & \sum_{v \in \mathcal{V}^{-i}} \int_{\mathbb{R}^{d-1}} \left( \int_{0^+}^{\infty} + \int_{-\infty}^{0^-} \right) (a_i \partial_{x_i} \Psi(x) + \lambda_i^+ - \lambda_i^-) f_i^- \exp(-\Psi(x)) dx_i \prod_{j \neq i} \rho(dx_j, v_j) \\ & + \sum_{v \in \mathcal{V}^{-i}} \left( \int_{\mathbb{R}^{d-1}} \left( \int_{0^+}^{\infty} + \int_{-\infty}^{0^-} \right) (-a_i \partial_{x_i} \Psi(x) + \lambda_i^- - \lambda_i^+) f_i^+ \exp(-\Psi(x)) dx_i \prod_{j \neq i} \rho(dx_j, v_j) \right) \\ & + \sum_{v \in \mathcal{V}^{-i}} \left( \int_{\mathbb{R}^{d-1}} a_i (f_i^+(0^+) - f_i^+(0^-)) \exp(-\Psi(x[i: 0])) \prod_{j \neq i} \rho(dx_j, v_j) \right) \\ & + \sum_{v \in \mathcal{V}^{-i}} \left( \int_{\mathbb{R}^{d-1}} -a_i (f_i^-(0^-) - f_i^-(0^+)) \exp(-\Psi(x[i: 0])) \prod_{j \neq i} \rho(dx_j, v_j) \right) \\ & + \sum_{v \in \mathcal{V}^{-i}} \left( \int_{\mathbb{R}^{d-1}} a_i (f_i^+(0^-) - f_i^+(0^+)) \exp(-\Psi(x[i: 0])) \prod_{j \neq i} \rho(dx_j, v_j) \right) \\ & + \sum_{v \in \mathcal{V}^{-i}} \left( \int_{\mathbb{R}^{d-1}} -a_i (f_i^-(0^+) - f_i^-(0^-)) \exp(-\Psi(x[i: 0])) \prod_{j \neq i} \rho(dx_j, v_j) \right) = 0, \end{aligned}$$

where we used that  $-v_i \partial_i \Psi(x) + \lambda_i(x, v) - \lambda_i(x, F_i(v)) = 0$ ,  $\forall (x, v) \in E$ .

#### A.5.2 Invariant measure of the sticky Bouncy particle process

Consider here the sticky  $d$ -dimensional Bouncy particle process described in Section 2.2.

The transition kernel  $R_\Psi(x)$  satisfies the following properties:

$$\langle \nabla \Psi(x), R_\Psi(x, v)v \rangle_\alpha = -\langle \nabla \Psi(x), v \rangle_\alpha$$

and

$$\|R_\Psi(x, v)v\|^2 = \|v\|_{\alpha^c}^2 + \|R_\Psi(x, v)v\|_\alpha^2 = \|v\|_{\alpha^c}^2 + \|v\|_\alpha^2 = \|v\|^2$$

so,  $\rho(R_\Psi^A(x)v) = \rho(v)$  ( $\rho(x)$  here denotes the standard Gaussian density evaluated at  $x$ ). Furthermore  $\lambda$  satisfies

$$\langle v, \nabla \Psi(x) \rangle_\alpha + \lambda(x, v) - \lambda(x, R_\Psi(x, v)v) = 0, \quad \forall (x, v) \in E. \quad (\text{A.2})$$

Let us check that the process satisfies  $\int \mathcal{L}f(x, v)\mu(dx, dv) = 0$ , for all  $f \in D = \{f \in C_c^1(E), \mathcal{A}f \in C_b(E)\}$  where  $\mathcal{L}$  is the extended generator  $\mathcal{A}$  given in Section (2.2) restricted to  $D$ .

First let us fix some notation: denote  $f_i(y) = f(x[i: y], v)$ ,  $Rf(x, v) = f(x, R_\Psi(x, v)v)$  and  $R\lambda(x, v) = \lambda(x, R_\Psi(x, v)v)$ . Also write  $\delta_0(dx_i, v_i) := \mathbb{1}_{v_i < 0}\delta_0^+(dx_i) + \mathbb{1}_{v_i > 0}\delta_0^-(dx_i)$  and  $\Delta_i f(x, v) := f(x[i: 0^+], v) - f(x[i: 0^-], v)$ . We have this preliminary result:

$$\begin{aligned} \int \sum_{i=1}^d \mathcal{G}_i f d\mu &= \frac{1}{C} \sum_i \int \left( \mathcal{G}_i f \exp(-\Psi(x))(dx_i + \frac{1}{\kappa_i}\delta_0(dx_i)) \right) \prod_{j \neq i} \left( dx_j + \frac{1}{\kappa_j}\delta_0(dx_j, v_j) \right) \rho(v) dv \\ &= \frac{1}{C} \sum_i \int (v_i \partial_{x_i} f \exp(-\Psi(x)) dx_i + v_i \Delta_i f \exp(-\Psi(x)) \delta_0(dx_i)) \prod_{j \neq i} \left( dx_j + \frac{1}{\kappa_j}\delta_0(dx_j, v_j) \right) \rho(v) dv \end{aligned} \quad (\text{A.3})$$

$$= \frac{1}{C} \sum_i \int (v_i \partial_{x_i} \Psi(x) f(x, v) \exp(-\Psi(x)) dx_i) \prod_{j \neq i} \left( dx_j + \frac{1}{\kappa_j}\delta_0(dx_j, v_j) \right) \rho(v) dv \quad (\text{A.4})$$

$$\begin{aligned} &= \frac{1}{C} \sum_{A \subset \{1, \dots, d\}} \left( \sum_{i \in A} \left( \int v_i \partial_{x_i} \Psi(x) f(x, v) \exp(-\Psi(x)) dx_A \right) \prod_{j \in A^c} \frac{1}{\kappa_j} \delta_0(dx_j, v_j) \right) \\ &= \frac{1}{C} \sum_{A \subset \{1, \dots, d\}} \int \langle v, \nabla \Psi(x[A^c: 0]) \rangle_A f(x[A^c: 0], v) \exp(-\Psi(x[A^c: 0])) dx_A \prod_{j \in A^c} \frac{1}{\kappa_j} \rho(v) dv \end{aligned} \quad (\text{A.5})$$

Here from (A.3) to (A.4) we used integration by parts in the two half planes  $(\infty, 0^+]$  and  $[0^-, -\infty)$ . For the equivalence of (A.4) to (A.5) note that placing  $|A|$  balls in  $d$  numbered boxes and marking one of them (say the ball in box  $i$ ) is equivalent to placing a marked ball in box  $i$  and distributing the remaining unmarked balls over the remaining boxes. Also notice that

$$\begin{aligned} \int \lambda_{\text{ref}} \int f(x, w) - f(x, v) \varrho(w) dw d\mu &= \\ \frac{1}{C} \sum_{A \subset \{1, 2, \dots, d\}} \lambda_{\text{ref}} \int (f(x, w) - f(x, v)) \exp(-\Psi(x)) dx_A \\ &\quad \times \prod_{i \in A^c} \frac{1}{\kappa_i} \delta_{0^-}(dx_i) \mathbb{1}_{v_i > 0} \mathbb{1}_{w_i > 0} 2^{|A^c|} \rho(v) \rho(w) dv dw \\ &+ \frac{1}{C} \sum_{A \subset \{1, 2, \dots, d\}} \lambda_{\text{ref}} \int (f(x, w) - f(x, v)) \exp(-\Psi(x)) dx_A \\ &\quad \times \prod_{i \in A^c} \frac{1}{\kappa_i} \delta_{0^+}(dx_i) \mathbb{1}_{v_i < 0} \mathbb{1}_{w_i < 0} 2^{|A^c|} \rho(v) \rho(w) dv dw, \end{aligned}$$

which is equal to 0 by symmetry between  $v$  and  $w$ . Then

$$\begin{aligned} \int \mathcal{L}f d\mu &= \frac{1}{C} \sum_{A \subset \{1, \dots, d\}} \int \langle v, \nabla \Psi(x[A^c : 0]) \rangle_A \exp(-\Psi(x[A^c : 0])) f(x[A^c : 0], v) dx_A \prod_{j \in A^c} \frac{1}{\kappa_j} \rho(v) dv \\ &\quad + \int (\lambda(x, v) - \lambda(x, R_\Psi(x, v))) f(x, v) \mu(dx, dv) \\ &= \frac{1}{C} \sum_{A \subset \{1, \dots, d\}} \int \langle v, \nabla \Psi(x[A^c : 0]) \rangle_A \exp(-\Psi(x[A^c : 0])) f(x[A^c : 0], v) dx_A \prod_{j \in A^c} \frac{1}{\kappa_j} \rho(v) dv \end{aligned} \quad (\text{A.6})$$

$$\begin{aligned} &+ \frac{1}{C} \sum_{A \subset \{1, \dots, d\}} \int (\lambda(x[A^c : 0], v) - \lambda(x[A^c : 0], R_\Psi v)) f(x[A^c : 0], v) \exp(-\Psi(x[A^c : 0])) dx_A \\ &\quad \times \prod_{j \in A^c} \frac{1}{\kappa_j} \rho(v) dv \\ &= 0, \end{aligned} \quad (\text{A.7})$$

where in equations (A.6)-(A.7) we used a change of variable  $v' = R_\Psi(x, v)v$  and property (A.2).

### A.5.3 Invariant measure of the $d$ -dimensional Boomerang process

The extended generator of the sticky  $d$ -dimensional Boomerang process is given by

$$\mathcal{A}f(x, v) = \sum_{i=1}^d \mathcal{G}_i f(x, v) + \lambda(x, v)(f(x, R_U(x, v)v) - f(x, v)) + \lambda_{\text{ref}} \int (f(x, w) - f(x, v)) \varrho_{x,v}(w) dw$$

and

$$\mathcal{G}_i f(x, v) = \begin{cases} |v_i| \kappa_i (f(T_i(x, v)) - f(x, v)) & (x, v) \in \mathfrak{F}_i \\ v_i \partial_{x_i} f(x, v) + x_i \partial_{v_i} f(x, v) & \text{else,} \end{cases}$$

where

$$\varrho_{x,v}(w) = \rho(w_{\alpha(x,v)}) \prod_{i \in \alpha(x,v)^c} 2\rho(w_i) \mathbb{1}_{v_i w_i > 0},$$

$\rho(y)$  being the standard normal density function evaluated at  $y$  and for sufficient regular functions  $f: E \rightarrow \mathbb{R}$  in the extended domain of the generator. Then, define  $D = \{f \in C_c^1(E), \mathcal{A}f \in C_b(E)\}$  and  $\mathcal{L}$  as the extended generator  $\mathcal{A}$  restricted to  $D$ . The component of the extended generator  $(x, v) \rightarrow \partial_{x_i} f(x, v) + x_i \partial_{v_i} f(x, v)$  produces Hamiltonian dynamics (see equation (2.7)) preserving any Gaussian measure centered on 0. Notice that the  $R_U(x)$  satisfies

$$\langle \nabla U(x), R_U(x)v \rangle_{\alpha(x,v)} = -\langle \nabla U(x), v \rangle_{\alpha(x,v)}$$

and that

$$\|\Sigma^{-1/2} R_U(x)v\| = \|\Sigma^{-1/2} v\|.$$

Then one can check that  $\int \mathcal{L}f(x, v) \mu(dx, dv) = 0$  by carrying out similar computations as in Appendix A.5.2.

## B Logistic regression example

Similar computations for the bounds of the Poisson rates of the Zig-Zag sampler applied to logistic regressions can be found in the supplementary material of Bierkens, Fearnhead, and Roberts (2019). Given a posterior density of the form of equation (1.2) with

$$\Psi(x) = \sum_{j=1}^N \left( \log \left( 1 + e^{\langle A_{[j,:], x} \rangle} \right) - y_j \langle A_{[j,:], x} \rangle \right) + \frac{1}{2\sigma^2} \|x\|^2$$



we use the sticky Zig-Zag subsampler presented in Section 3. To that end, define  $U(x) = \Psi(x) - \frac{1}{2\sigma^2}\|x\|^2$ . We decompose the partial derivatives of  $U$  as follow:

$$\partial_{x_i}U(x) = \sum_{j \in \Gamma_i} S(x, i, j)$$

with sets  $\Gamma_i = \{j \in \{1, 2, \dots, N\} : A_{j,i} \neq 0\}$  and

$$S(x, i, j) = \left( \frac{A_{[j,i]} e^{\langle A_{[j,:],x} \rangle}}{1 + e^{\langle A_{[j,:],x} \rangle}} - y_j A_{[j,i]} \right).$$

Then, for  $J \sim \text{Unif}(\Gamma_k)$ , the estimator  $S_J[|\Gamma_i|(S(x, i, J) - S(x^*, i, J)) + \partial_{x_i}U(x^*) + \sigma^{-2}x_i]$  is unbiased for  $\partial_{x_i}\Psi(x)$ . First of all, notice that the partial derivative of  $S(x, k, j)$  is bounded:

$$\partial_{x_i}(S(x, k, j)) = \frac{A_{[j,k]}A_{[j,i]}e^{\langle A_{[j,:],x} \rangle}}{(1 + e^{\langle A_{[j,:],x} \rangle})^2} \leq \frac{1}{4}A_{[j,k]}A_{[j,i]},$$

which means that for  $i = 1, 2, \dots, d$

$$|S(x, i, j) - S(x', i, j)| \leq C_i \|x - x'\|_p, \quad p \geq 1, j \in \Gamma_i, x, x' \in \mathbb{R}^d,$$

with

$$C_k = \frac{1}{4} \max_{j=1,\dots,N} |A_{[j,k]}| \|A_{j,:}\|_2.$$

Then given an initial position  $(x, v) \in E$ , tuning parameter  $x'$  and for any  $t \geq 0$ , write  $(x(t), v(t)) = \varphi(t, x, v)$  with  $i \in \alpha(x, v)$  :

$$\begin{aligned} \tilde{\lambda}_i(x(t), v(t)) &= (v_i (\partial_{x_i}U(x') + \sigma^{-2}x_i(t) + \Gamma_i(S(x(t), i, j) - S(x', i, j))))^+ \\ &\leq (v_i(\partial_{x_i}U(x') + \sigma^{-2}(x_i + v_i t)))^+ + |v_i|\Gamma_i(|S(x(t), i, j) - S(x, i, j)| + |S(x, i, j) - S(x', i, j)|) \\ &\leq (v_i(\partial_{x_i}U(x_{ref}) + \sigma^{-2}(x_i + v_i t)))^+ + |v_i|\Gamma_i C_i (t\|v\|_p + \|x - x'\|_p). \end{aligned}$$

Thus we set

$$\lambda_i(t, x, v) = v_i(a_i(x, v) + b_i(x, v)t)$$

where  $a_i(x, v) = v_i(\partial_i U(x') + \sigma^{-2}x_i)^+ + C_i \Gamma_i |v_i| \|x - x'\|_p$  and  $b_i(x, v) = |v_i| C_i \Gamma_i \|v\|_p + v_i^2 \sigma^{-2}$ . We choose  $x'$  to be the posterior mode of  $\exp(-\Psi)$ , which in this case is unique and easily found with the Newton's method since the function  $\exp(-\Psi)$  is convex.

Given an initial position  $(x, v)$ , suppose the particle  $j \neq i$  gets frozen at time  $\tau \geq 0$ . Then for  $t \geq \tau$  we have that  $\|\int_0^t v(t)dt\|_p = \tau\|v\|_p + (t - \tau)\|v'\|_p \leq t\|v\|_p$ , with  $v' = v[j:0]$ . This implies that the Poisson times drawn before the  $j$ th coordinate gets stuck are still valid upper bounds after time  $\tau$ . The same argument follows easily for  $n \geq 1$  coordinates getting stuck at 0.

## C Computationally challenging example

As a benchmark for comparisons, we report the detailed results obtained when running the sticky Zig-Zag sampler with local implementation in a challenging scenario of a high dimensional parameter space ( $\approx 100,000$ ). The experiment was performed with a conventional laptop with a 2.3GHz Intel core i6-6770HQ processor and 8GB DDR4 RAM and can be reproduced in <https://github.com/mschauer/ZigZagBoomerang.jl/blob/master/research/sticky/heart/heartextra.jl>. For this example, we do not compare the sticky Zig-Zag sampler with the standard Zig-Zag sampler since the latter algorithm does not return the output within 30 minutes.

We consider the example outlined in Section 5.2 with  $n \times n$  pixels. We chose  $n = 300$  and used the ground truth to be the heart function of Section 5.2 with 90% of pixels outside the region of interest (see Figure 9). We assume to observe each pixel corrupted with with noise (Figure 10, top-left panel).

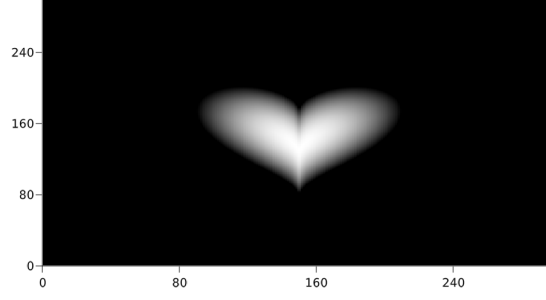


FIGURE 9: Ground truth: heart function presented in Section 5.2, with 90% of black pixels which are outside the region of interest.

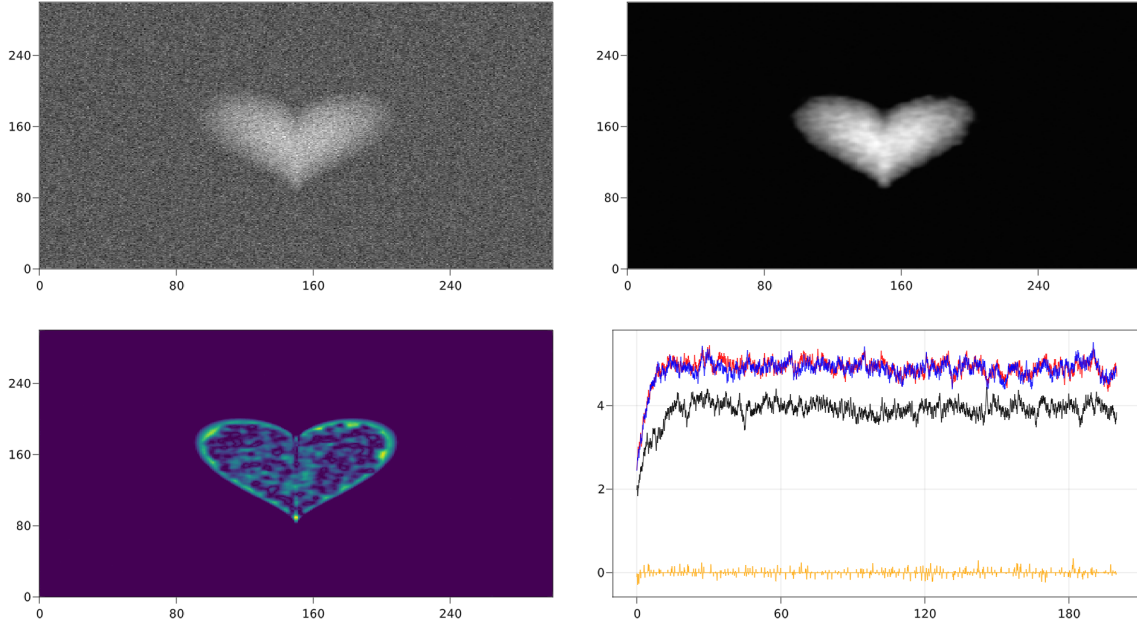


FIGURE 10: Top-left: observed image of the heart corrupted with white noise. Top-right: posterior mean estimated from the trace of the sticky Zig-Zag sampler. Bottom-left: image showing the error between the posterior mean and the ground truth. Top-right: trace plot of 4 coordinates. The traces marked with red and blue lines belong to neighbouring coordinates (highly correlated) the trace marked with yellow, belongs to a coordinate outside the region of interest.

Here the prior is chosen to be

$$\mu_0(dx) \propto c_1 \Lambda^2 + c_2 I \prod_{k=1}^{n \times n} \left( dx_k + \frac{1}{\kappa} \delta_0(dx_k) \right)$$

with  $\Lambda$  defined as in Section 5.2,  $c_1 = 10.0$ ,  $c_2 = 0.1$  and  $\kappa = 2$ . Taking a power of the Laplacian amounts to imposing stronger prior smoothness, making the neighbouring pixels a priori and a posteriori stronger correlated (see the red and blue lines in Figure 10, bottom-right, for the traces of two neighbouring pixels). This makes the sampling problem more difficult, adding to the challenge.

We set the set of velocities  $\mathcal{V} = \{-1, +1\}^d$  and the final clock of the sticky Zig-Zag sampler to 200. The algorithm runs for  $\approx 930$  seconds and returns the skeleton of points as described in Section 4 from which we can efficiently estimate the posterior mean (this last step takes  $\approx 22$  seconds). The sum of the errors between the posterior mean and the ground truth is 2876.